CONTROL OF SUPERCONDUCTING MACHINES FOR SHIP PROPULSION

AUTHOR: LOUIS S. MATJASKO

SUPERVISOR: H. H. WOODSON

DATE SUBMITTED: 17 MAY 1968

CONTROL OF SUPERCONDUCTING MACHINES FOR SHIP PROPULSION

by

LOUIS STEPHEN MATJASKO

LIEUTENANT, UNITED STATES NAVY

B.S., United States Air Force Academy

(1963)

Submitted in Partial Fulfillment of the

Requirements for the Degree of

Naval Engineer and the Degree of

Master of Science in Electrical Engineering

at the

MASSACHUSETTS INSTITUTE OF TECHNOLOGY

May, 1968

ABSTRACT

Control of Superconducting Machines for Ship Propulsion

Louis S. Matjasko

Submitted to the Department of Naval Architecture and Marine Engineering on 17 May 1968 in partial fulfillment of the requirements for the Master of Science degree in Electrical Engineering and the Professional Degree, Naval Engineer.

It is known that superconducting machines of capacity large enough to power ships of a destroyer's size are within the capability of present technology. Given this fact, the control of these machines must be examined to the extent of determining ship performance realizable with such a drive system.

A mathematical model for ship-propulsion plant performance is derived using the propeller characteristics of Nordstrom [14]. From the model, a set of ideal performance characteristics in the form of plots of stop to full ahead and crash astern transients is obtained. These do not account for any equipment, prime mover, or machine limitations.

A conceptual design of a control system is presented. The system accounts for limitations on ideal performance that are discussed. Feasibility of the system is demonstrated.

Finally, incorporating the limitations to ideal performance, the model and control system are used to predict realistic ship performance characteristics, assuming power plants of gas turbines and conventional steam.

The principal results are that the gas turbine plant provides faster response to demands for increasing speed and that neither plant provides an advantage in a crash astern maneuver.

The characteristic plots for the transient maneuvers provide a basis of comparison for the observer familiar with capabilities of other power plant, control, and drive system combinations.

Thesis Supervisor: Herbert H. Woodson

Title: Professor of Electrical Engineering

TABLE OF CONTENTS

LIST OF SYMBOLS

T_t - Total propeller thrust (lbs)

R_t - Total ship resistance (lbs)

a -- Added mass coefficient

Δ - Ship displacement (tons)

g - Acceleration of gravity (ft/sec^2)

v_s - Ship speed (ft/sec)

v - Propeller speed of advance (ft/sec)

t - Time (sec)

n - Shaft speed (rev/sec)

w - Wake fraction

μ - Thrust deduction

λ - Propeller advance coefficient

D - Propeller diameter (ft)

P - Propeller pitch (ft)

ρ - Water density $(\frac{lb\ sec^2}{ft^4})$

Q_e - Total electromagnetic torque (ft-lbs)

Q_p - Required propeller torque (ft-lbs)

Q_f - Frictional torque

J - Rotational moment of inertia (ft-lb sec^2)

I_f - Amplitude of field current

I_{pk} - Amplitude of stator current per phase

L_{sr} - Amplitude of rotor-stator mutual inductance

α - Angle between rotor and stator magnetic axes

$\underline{E}$ - Synchronous voltage (complex amplitude)

ω - Shaft angular velocity (rad/sec)

M_s - Stator to stator mutual inductance

L_s - Stator self inductance

ϕ - Power factor angle

$\underline{V}$ - Motor terminal voltage (complex amplitude)

R - Resistance, electrical

INTRODUCTION

Traditionally, installation of an electric propulsion system on a ship has imposed a weight, volume, and cost penalty. A major part of this penalty is due to the control system components as well as the machines themselves [17].

Developments in solid state rectifier electronics have greatly enhanced the flexibility of electric propulsion and made possible lower weight and volume control systems [17]. In addition, low temperature technology can make it possible to realize weight and volume savings in the machinery itself.

Coupling these developments into a solid-state superconducting electric drive system will then provide overall substantial weight and volume savings. This may well overcome one of the shortcomings of electric drives. It remains to be seen whether costs of such a system would be less than those of a conventional electric drive.

In the past, geared turbine plants have had the weight, volume, and cost advantage over electric plants [17]. However, electric drive, and especially a solid-state superconducting electric drive, provides more rapid response for better maneuverability. Solid-state rectifier control provides this capability at all speeds.

It is the purpose of this report to conceptually design and evaluate the ship performance attainable with a solid-state control system and synchronous generators and motors with superconducting rotors and nonsuperconducting armatures. The control system employs a silicon controlled rectifier cycloconverter.

PROCEDURE

The essential steps followed in this report are:

1. Development of an adequate mathematical model for ship-propulsion plant interaction using suitable propeller characteristics.

2. Evaluation of ideal ship performance characteristics employing the model.

3. From a study and understanding of the ideal characteristics and assumptions, proposal of a conceptual design of a control system that would account for equipment and power plant limitations on ideal performance.

4. Inclusion of these limitations and use of the model in the evaluation of final performance characteristics.

SHIP-PROPULSION PLANT MODEL DEVELOPMENT

The objective of the model is to predict reasonably the behavior of the ship-propulsion system in order that valid decisions regarding control of the system can be made.

Ship Motion

Motion of the ship can be described in general by Newton's Law of Motion:

$$T_t - R_t = (1 + a) \frac{\Delta}{g} 2240 \frac{dv_s}{dt} \qquad (1)$$

For this analysis, $R_t = K v_s^2$ is assumed. Added mass is assumed to be .08. Ship displacement is 3700 tons.

It is recognized that at lower speeds the resistance approximation is reasonable. However, at higher speeds, a cubic may more accurately approximate the resistance. Therefore, inaccuracies will occur in computation of transients with this model. This is discussed at the end of this section.

Total propeller thrust is a function of ship speed and shaft speed. However, propeller characteristics for thrust and torque are plotted as functions of speed of advance and shaft speed. Speed of advance is related to ship speed by:

$$v = (1 - w) v_s$$

Henceforth, this report will be in terms of v.

Wake fraction is a function of hull geometry and ship speed. It expresses the interaction between the water flow and the ship's hull.

The hull effectively reduces the velocity of the water seen by the propeller.

Similarly, there is a hull interaction affecting thrust. A propeller provides thrust, T, but there is available only an amount $(1 - \mu)T$ to overcome ship resistance.

To further define thrust, use of propeller characteristics developed by Nordstrom, [14], will be made. These consist of non-dimensional plots of thrust and torque versus λ, advance coefficient. λ is given by:

$$\lambda = \frac{v}{nD}$$

Since the characteristics are plotted as a function of v, wake fraction must be known. For this report, wake fraction and thrust deduction are assumed as constant for the sake of simplification of calculations. The true nature of system behavior will not be betrayed by this assumption and accuracy of results will not be significantly affected. Again, precise results are not the objective of the model, but only a reasonable prediction of system behavior. Constant w and μ were assumed for such a model in [13].

Given D and v_{max}, using Nordstrom characteristics, one can make a plot of $T/\rho D^4$ versus n for v = constant = v_{max}. Such a plot is shown in Figure I. Also shown is the model for thrust which is given by:

$$T(v,n) = - C_1 v^2 + D_1 n^2$$

Figure I

Nordstrom and model propeller thrust versus n with $v = v_{max}$ for one propeller. P/D = 1.0

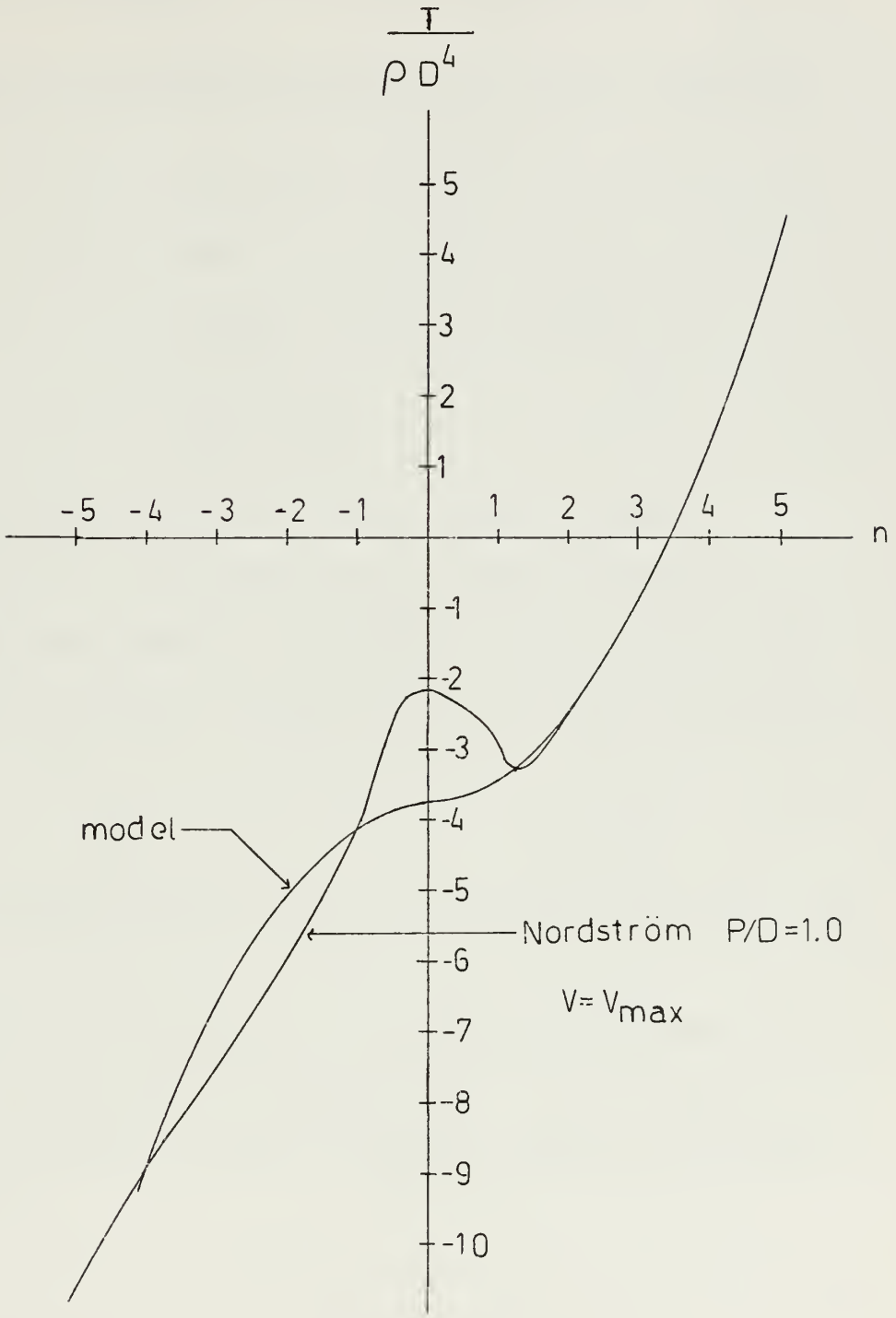

The equation of motion now becomes:

$$(1.08)\ 2240\ \frac{\Delta}{g}\ \frac{dv}{dt} = (1 - \mu)\ [-C_1 v^2 + D_1 n^2] - K\ v^2 \qquad (1a)$$

Other ship and propeller parameters not mentioned above are:

$$D = 13.25$$

$$n_{max} = 5$$

$$v_{s\ max} = 33 \text{ kts} = 55.7 \text{ ft/sec}$$

$$w = \mu = .1$$

$$P/D = 1.0$$

Maximum horse power for each of the two shafts is 35,000.

In Appendix A, the constants C_1, D_1, and K are evaluated. Substituting those values and simplifying equation (1a), the model equation for ship motion is obtained in equation (2). The absolute value

$$\frac{dv}{dt} = -1.25\ 8 \times 10^{-3}\ |v|v + .1265\ |n|n \qquad (2)$$

signs are necessary for the cases of negative ship speed and/or shaft speed.

Although, as seen in Figure I, the thrust model begins to deviate somewhat from the Nordstrom propeller for $n < 2$, it is felt that with general consideration the model is accurate enough for the analysis to be performed.

Shaft Motion

Newton's Law again applies for shaft motion. Equation (3) represents torques for

$$2(2\pi J)\frac{dn}{dt} = Q_e - Q_p - Q_f \tag{3}$$

two shafts and two-shaft motion. J represents propeller and entrained water inertia plus the inertia of the motor rotor. In this analysis, it is assumed that Q_f is small enough to be considered negligible in comparison with the other torques involved. Nordstrom characteristics are again used to define Q_p. Figure II is a plot of $Q_p/\rho D^5$ versus n with $v = v_{max}$ for both the Nordstrom propeller with P/D = 1.0 and the model torque. Q_p is modeled as follows:

$$Q_p = A\,n^2 - B\,v^2 \tag{4}$$

In Appendix A, A, B, and J are computed. The equation for shaft motion, with substitution for A, B, and J and rearranging, becomes:

$$\frac{dn}{dt} = .93 \times 10^{-5}\,Q_e - .785\,|n|n + 3.29 \times 10^{-3}\,|v|v \tag{5}$$

Equation (5) represents two-shaft operation. It is considered an adequate model for the purposes of this analysis.

With regard to the approximation of ship's resistance as $K\,v_s^2$, the transients to be computed will be less accurate. For the stop to full ahead transient, the model will predict a faster transient due to the lower R_t than actually exists at high speeds. The model will predict a longer stopping transient from high speeds due to the smaller R_t assumed. This must be kept in mind when evaluating results.

Figure II

Nordstrom and model propeller torque versus n with $v = v_{max}$ for one propeller. P/D = 1.0.

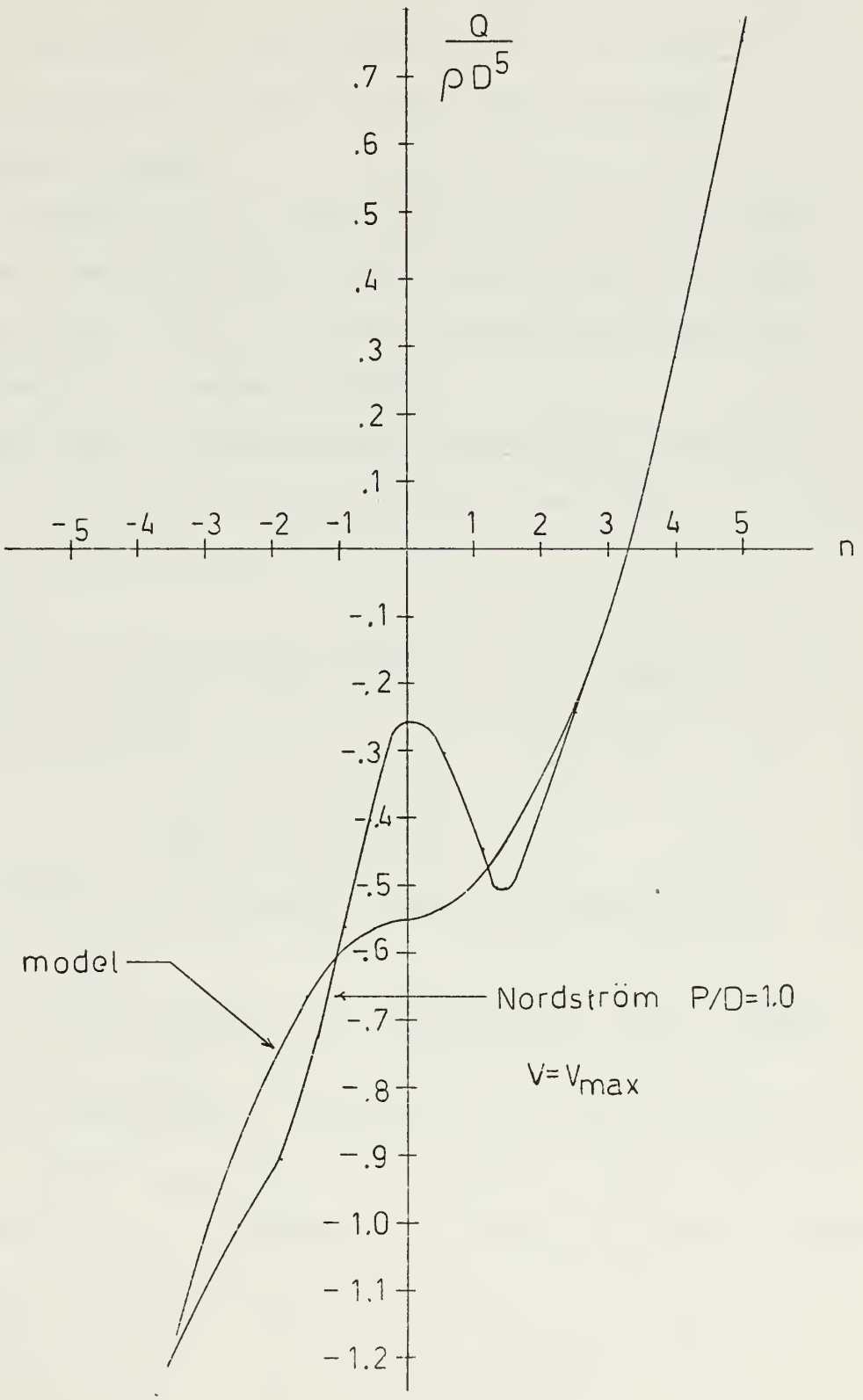

IDEAL SYSTEM TRANSIENTS

Using the model as expressed by equations (2) and (5), the stop to full ahead transient and the crash astern transient are computed and discussed. These transients assume no prime mover limitations.

Stop to Full Ahead Transient

For this transient, it is assumed that the shaft will have reached a steady state value of revolutions before the ship's speed has changed an appreciable amount. This is a realistic assumption for this ship. The system equations then become decoupled.

Full motor torque is assumed applied immediately upon command from the bridge. This torque can be maintained for as long as desired or until a desired ship speed is reached.

Shaft Transient

Assuming v = 0, the shaft motion equation becomes equation (6), since $Q_{e\ max} = 12.24 \times 10^5$ ft-lbs.

$$\frac{dn}{dt} = 11.38 - .785\ n^2 \tag{6}$$

Separation of variables and standard integration technique yields:

$$t = \int_0^{\bar{n}_1} \frac{dn}{11.38 - .785\ n^2} = \frac{1}{\sqrt{11.38\ (.785)}} \tanh^{-1}\left[n_1 \sqrt{\frac{.785}{11.38}}\right] \tag{7}$$

This solution is valid until $n_1 = 3.8$ and $t = 1.31$ seconds. At this point, with v = 0, Q_p equals $Q_{e\ max}$. Q_p is then constrained at this value since it cannot exceed $Q_{e\ max}$. The ship speed now begins to increase while shaft

speed is in the steady state as given by equation (8). As the ship

$$.785\ n^2 = 11.38 + 3.29 \times 10^{-3}\ v^2 \qquad (8)$$

increases speed due to the positive thrust of the propeller, the propeller required torque and thrust curves are continually shifting as indicated in Figures III and IV. Finally, when the ship reaches maximum speed, the curves are those of Figures I and II. Therefore, maximum n is not reached until maximum ship speed is attained. To complete this transient, the ship speed transient must be computed.

Ship Speed Transient

At t = 1.31 and n = 3.8, equations (2) and (8) become a coupled set. Solving equation (8) for n^2 and substituting in (2), one obtains equation (9).

$$\frac{dv}{dt} = 1.83 - .727 \times 10^{-3}\ v^2 \qquad (9)$$

The solution for t is that of equation (7) but with appropriate constants and v substituted for n_1. The solutions of equations (6), (8), and (9) are plotted in Figure V. As assumed, the shaft transient is much faster than the ship speed transient.

These results are based on additional assumptions:

1. The propellers are not cavitating
2. The propellers are fully immersed and not aerating
3. As a consequence of the above assumptions, in the steady state ($\frac{dn}{dt} = 0$) the propellers are transmitting the applied torque and power.

The second assumption is certainly valid since, under all normal operating conditions for a destroyer, the draft is sufficient and the location of the

Figure III

Nordstrom and model torque versus n with v as a parameter for one propeller. Dashed line is steady state v versus steady state n.

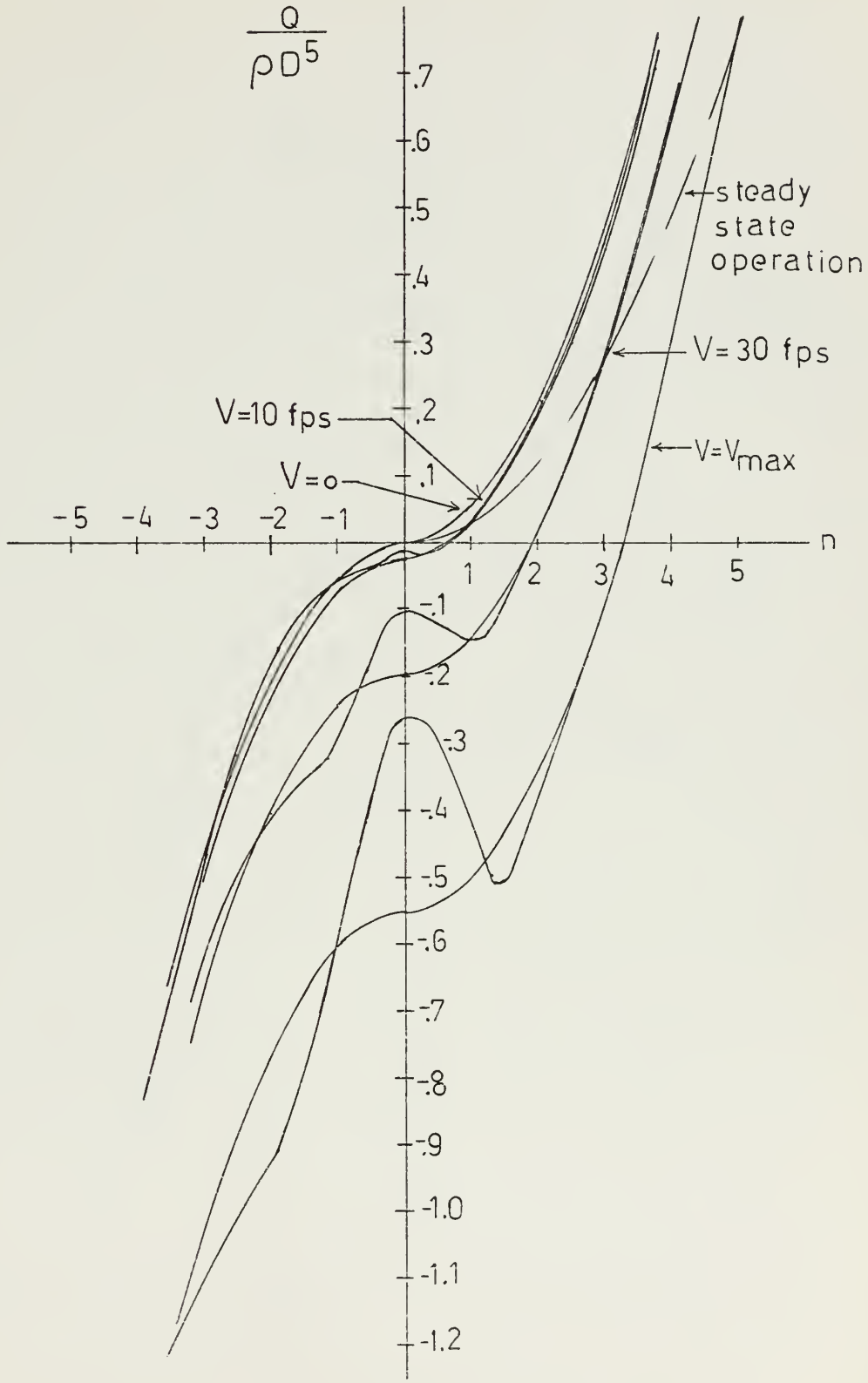

Figure IV

Nordstrom and model thrust versus n with v as a parameter for one propeller. Dashed line is steady state v versus steady state n.

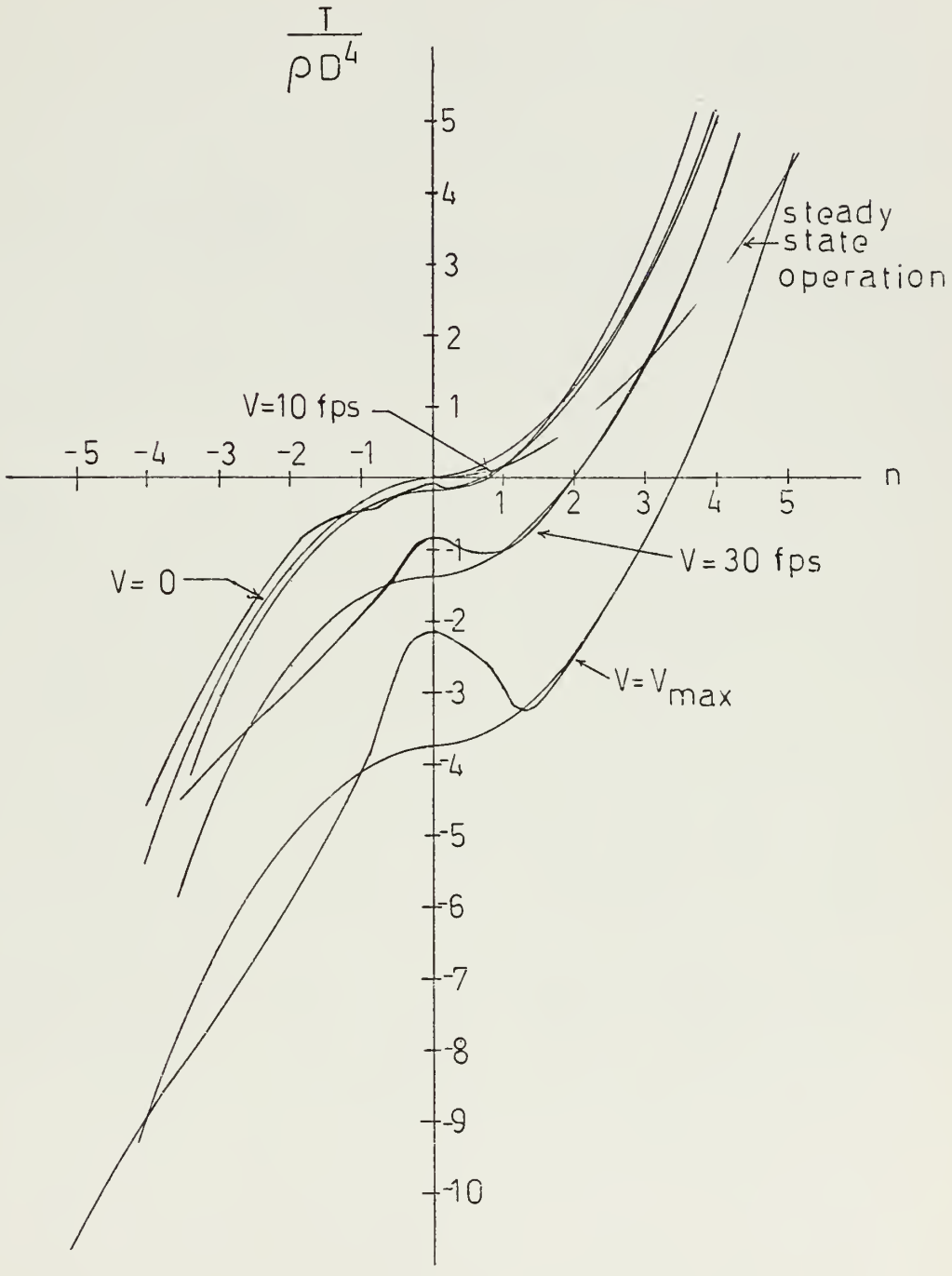

Figure V

Ideal stop to full ahead transient, including thrust and torque.

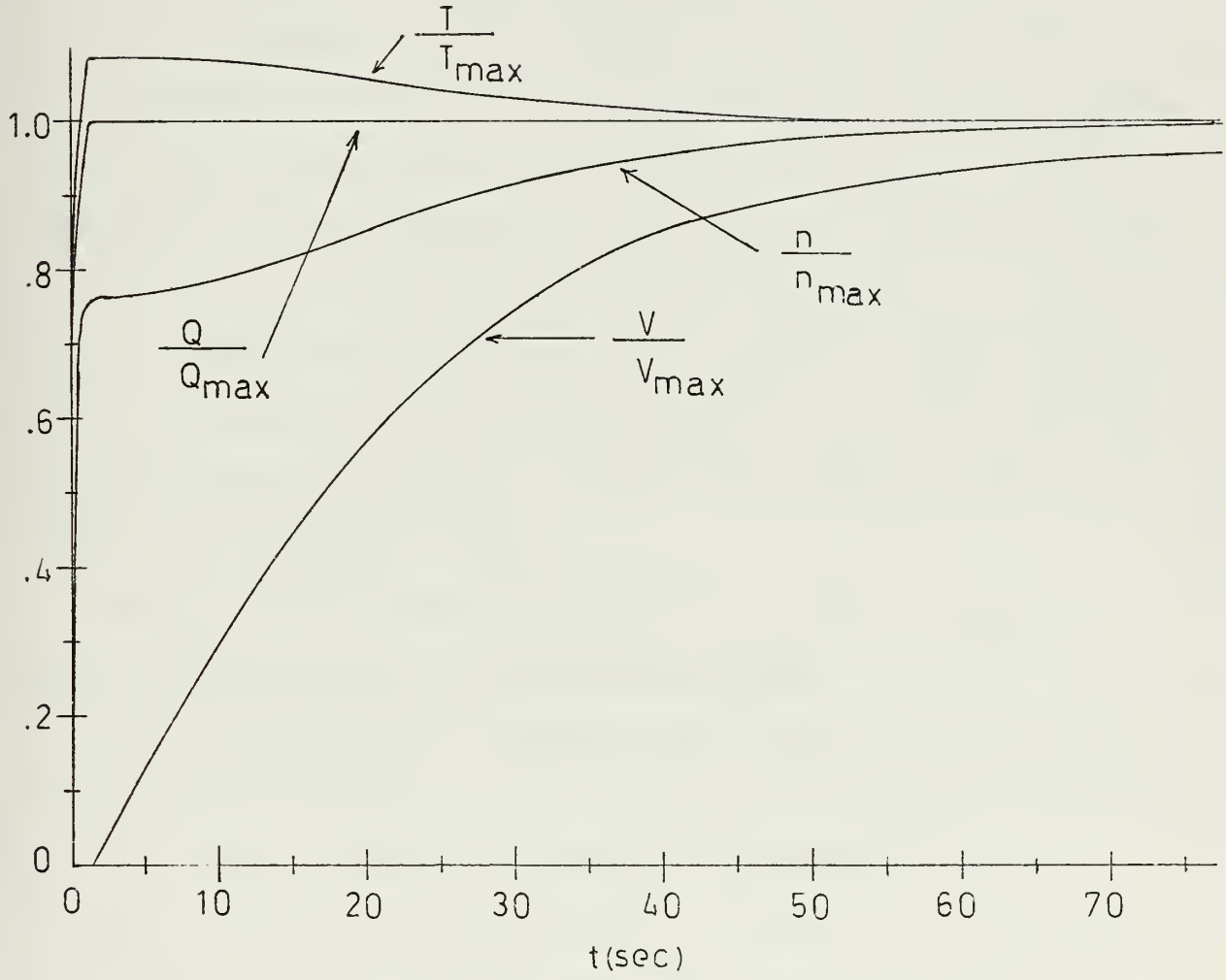

propellers is well under the stern such as to insure complete propeller immersion. This practically insures that air is not drawn down from the water surface. Aeration did not occur for the actual propeller tested by Nordstrom.

As for the first assumption, cavitation did not take place with the Nordstrom propeller. It is reasonable to assume generally that cavitation would not occur during an actual ship transient.

Nordstrom presents no information with regard to test pressure or cavitation number for the tests with which he characterized his propellers. At high ship speeds and low n, the propeller is likely to be in extreme stall where the pressure differential is not going to be adequate to cause cavitation. At these same speeds and higher n, cavitation is a much bigger threat to thrust breakdown. However, with the absence of any full scale data, it is assumed that cavitation has at most a very minor effect in the full scale situation modeled here. In any case, cavitation effects can be minimized by good propeller design.

Assumption three is then considered valid for this transient.

Control Aspects of the Stop to Full Ahead Transient

Prior to t = 0, the main propulsion motor and generator fields are excited with maximum field current. These are the superconducting windings, while the stators are non-superconducting. The generator is at rated voltage. At t = 0, the SCR cycloconverter controller must apply maximum motor torque. It must, therefore, pass rated current to the motor and maintain it. This again assumes no prime mover or generator limitations on such performance.

As derived in Chapter 6 of [11], the motor torque for a P-pole, balanced three phase smooth air gap machine is given by

$$Q_e = -\frac{3}{2}\left(\frac{P}{2}\right) I_f I_{pk} L_{sr} \sin \alpha \qquad (10)$$

The field current, I_f, is to be kept at its maximum for all maneuvers since it is not costly to do with superconductors. It also eliminates a control variable and contributes to maximum torque.

L_{sr} is a constant and a function of geometry. Stator internal resistance is neglected.

Stator current, I_{pk}, must be maintained at its maximum which is limited by thermal consideration.

The other control variable, then, is α. For maximum torque, and motor action, $\alpha = -90^{\circ}$. Maintaining this desired phase between rotor and stator magnetic field axes and I_{pk} at its maximum results in maximum torque. The phase relationship is pictured in Figure VI.

Figure VI

Motor configuration, 3 phase stator, single phase rotor.

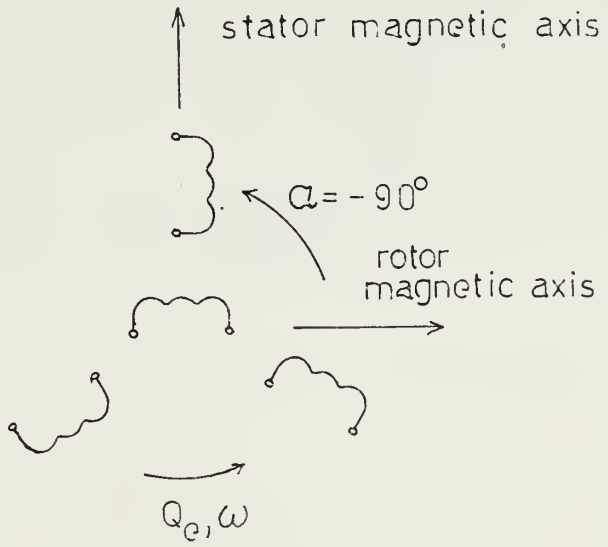

Crash Astern from Full Ahead Transient

The initial conditions for this transient are that ship speed, shaft speed, propeller and motor torque are at their maxima. At $t = 0$, full reverse electromagnetic torque is instantaneously applied to the shaft and maintained for the duration of the transient. Model and reversing torques are plotted in Figure VII.

Again, for ease of computation, it is assumed that the shaft transient is much faster than the ship speed transient. From Figure VII, it is seen that when $n \tilde{=} -2$, $\frac{dn}{dt} = 0$, and the ship speed begins decreasing.

With $v = v_{max}$ and $Q_e = -Q_{e\ max}$, the shaft transient is governed by equation (11).

$$\frac{dn}{dt} = -.785\ |n|n - 3.09 \tag{11}$$

Separating variables and integrating, one obtains for $n > 0$,

$$t = .642\ \tan^{-1}\ [\frac{n}{1.985}]_0^{n_1} \tag{11a}$$

When $n = 0$, $t = .766$ seconds. For $n < 0$, the sign modifying the first term on the right of equation (11) changes to plus. The solution, then, for the region $-1.985 < n < 0$ is

$$t = .321\ \ n\ [\frac{3.94 + 1.985\ n}{3.94 - 1.985\ n}]_0^{-n_2} \tag{11b}$$

Total time to reach $n = -1.98$ is 2.9 seconds. At this point, $\frac{dn}{dt} = 0$, $n < 0$, and equation (11) becomes

Figure VII

Model and reversing torques for crash astern, one propeller.

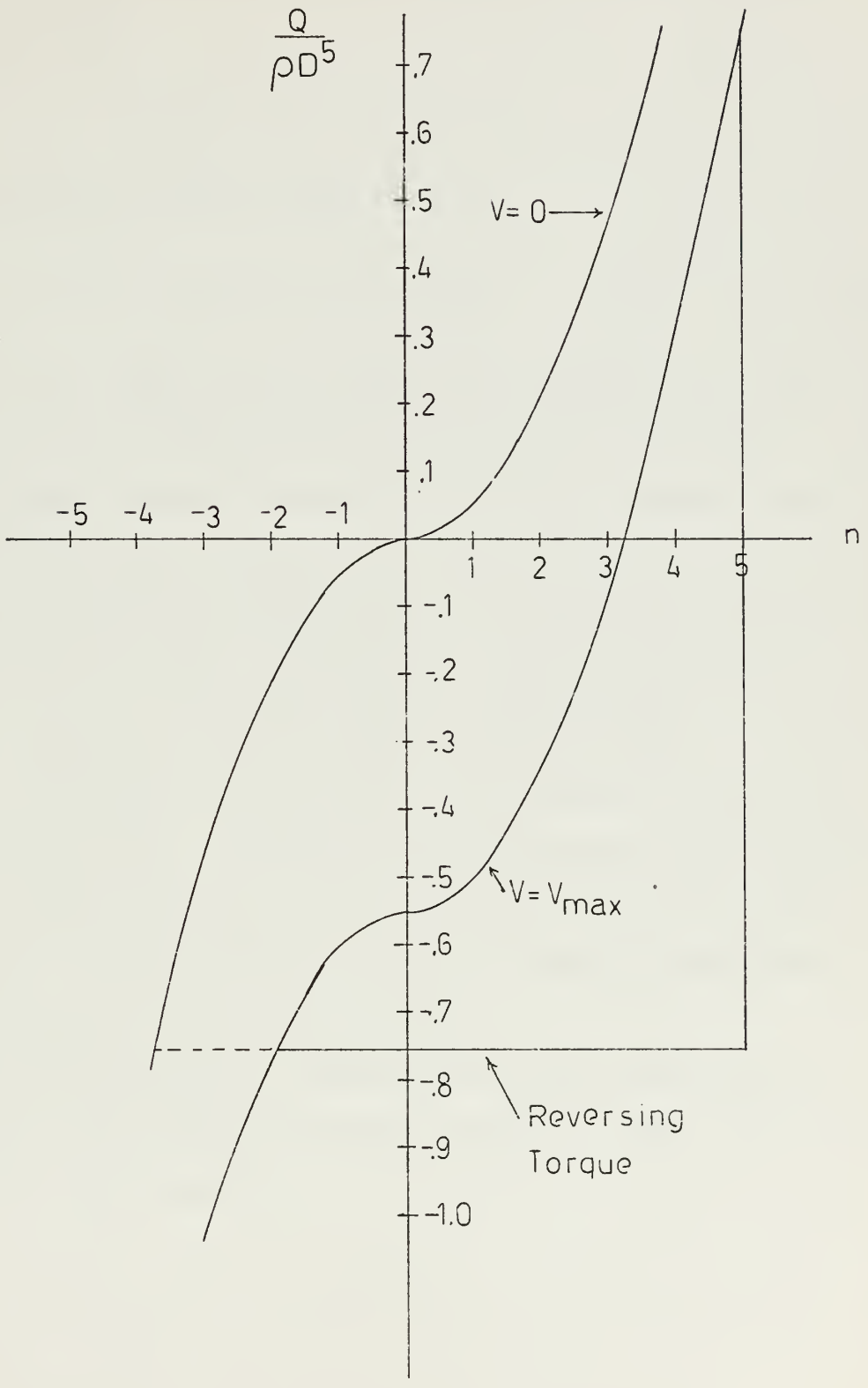

$$.785\ n^2 = 11.38 - 3.29 \times 10^{-3}\ v^2 \qquad (12)$$

Solving (12) for n^2 and substituting in (2), the ship speed equation becomes equation (12a).

$$\frac{dv}{dt} = -1.83 - .727 \times 10^{-3}\ v^2 \qquad (12a)$$

The solution to (12a) is similar to that of (11).

$$t = 27.45 \tan^{-1} \left[\frac{v}{50.15}\right] \qquad (12b)$$

The solutions, (11a), (11b), and (12b) are plotted in Figure VIII. It is seen that total time for this transient is approximately 25 seconds.

Here, the shaft transient is about 12% of the total transient time. For the stop to full ahead transient, the shaft portion was only about 2%. It is therefore reasonable that $\frac{dv}{dt}$ would not be insignificant over such a large portion of the transient, especially when true ship resistance is accounted for. This is an additional time shortening advantage.

Near n = 0, at higher ship speeds, there is a pronounced hump in the Nordstrom propeller curves. The propeller would decelerate faster than the model predicts through that region due to the greater deceleration torque acting. However, as seen in Figure II, for $n < -1$ there is actually less decelerating torque than predicted by the model.

Weighing the discrepancies in resistance and deceleration torque, it is felt that the results obtained for this transient are a fair representation of an ideal crash astern maneuver.

Figure VIII

Ideal crash astern transient, including thrust and torque.

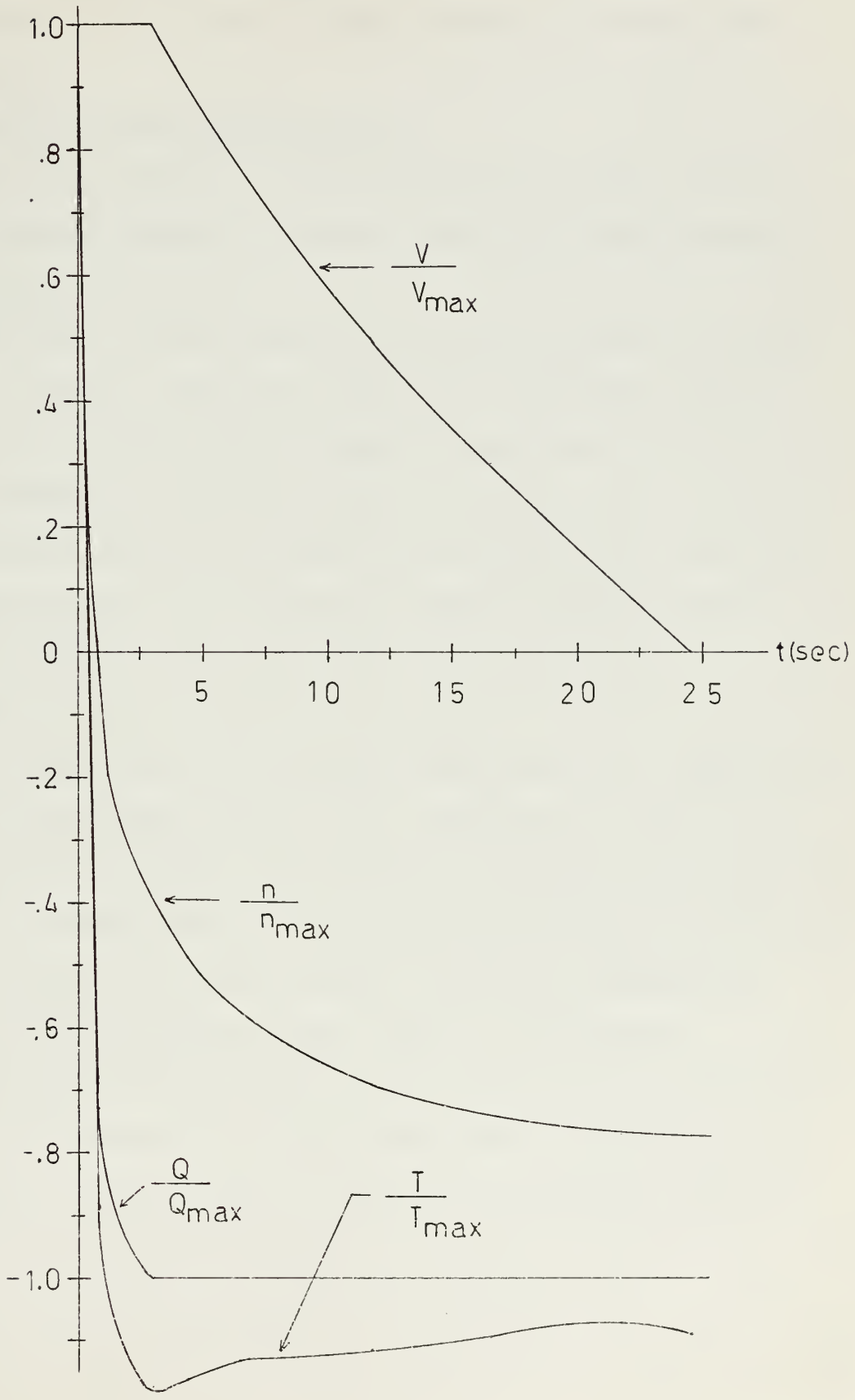

Another complication may be cavitation, but again this is assumed to have a negligible effect on performance.

The significance of the times for this transient is discussed under General Remarks.

Control Aspects of the Crash Astern Transient

To execute this transient, on command from the bridge the controller must reverse the motor torque to a maximum. This would be done by dynamic braking or reversing $\sin\alpha$ to +1.

While the shaft is still rotating in the positive direction, the motor is acting as a generator. Therefore, energy must be dissipated either in the main generator and motor or in an external dynamic braking resistor.

If it is desired to stop the ship dead in the water rather than pass through zero speed, as would be the case here, one would have to remove the reversing torque before $v = 0$. The point at which the torque is removed could be preprogrammed or most capably left to the seaman's eye.

General Remarks

These transients represent the extreme capabilities of the ideal electric motor, controller and model propeller. For a destroyer, one would like to have the capability of stopping and accelerating most quickly. Therefore, the objective of the control system is to make these extreme capabilities as nearly as possible available to the ship commander. Intermediate capabilities, maneuvering at other than maximum torque, should also be provided.

In designing the control system, it must be recognized that the immediate application of full torque from an idling state will be limited mechanically by the response of the prime mover to changing load requirements. Also, in

the crash astern maneuver, immediate removal of full load from the generator will cause the prime mover to speed up very rapidly. These are the main limitations that must be overcome for the attainment of desired ship performance.

At first glance, the time to stop the shaft in the crash astern maneuver seems phenomenal, since for geared turbine steam plants it usually requires from 20 to 30 seconds. The reason for this difference may be seen by making an energy accountability for the transient. For each drive system there is both rotational and hydrodynamic energy to be dissipated in stopping the shaft. For the electric drive, there is additional energy from the prime mover to be absorbed. This is assuming that the load is removed while the prime mover remains at full power.

The rotational energy is given by $1/2\ I\ \omega^2$, where I is the total rotating inertia. Hydrodynamic energy for the ideal transient is computed in Appendix B. If it is assumed that the shape of the shaft transient is the same for the geared turbine plant but extended in time by a factor of thirty, the hydrodynamic energy will be increased by a factor of thirty.

As derived in Appendix A, the rotational moment of inertia of one shaft for the electric drive is 8582 ft-lb sec^2. For the geared turbine plant of [7], which was 25,000 horsepower per shaft, the total rotational moment of inertia per shaft was 73,800 ft-lb sec^2. As an approximation, it is assumed that this is the same that exists in the ship under discussion with a 35,000 horsepower per shaft geared steam turbine plant. In actuality, it is probably somewhat less, which makes the following comparison more conservative.

Additional energy to be absorbed in the case of the electric drive here discussed is that absorbed by the variable load resistor during dynamic braking and motor plugging. This is assumed to be full power for two seconds. For the geared turbine drive this energy is negligible. Table I lists these energies for comparison.

Table I

Energies absorbed during crash astern for geared turbine and solid-state superconducting electric drives. Energy in joules.

	Hydrodynamic Energy	Rotational Energy=1/2 I ω^2	Additional Energy	Total
Electric	10.4×10^6	11.5×10^6	104.4×10^6	126.3×10^6
Geared Turbine	312×10^6	158.8×10^6	———	470.8×10^6

From Table I it is seen that total energy required to be removed for the superconducting electric drive is considerably less than for the conventional geared turbine drive. This accounts for the great difference in times to stop the shaft.

The rapid shaft transient coupled with the effects of ship resistance is the reason for the difference in ship starting and stopping times. Figure IX illustrates the advantage provided by this rapid shaft transient. Ship resistance is favorable to stopping the ship while it is not favorable to starting. Because the shaft transient is so rapid in crash astern the ship has remained essentially at its maximum speed. Shaft speed is negative and the propeller is producing greater than maximum thrust. This is the

Figure IX

Thrusts available from one propeller
in starting and stopping.

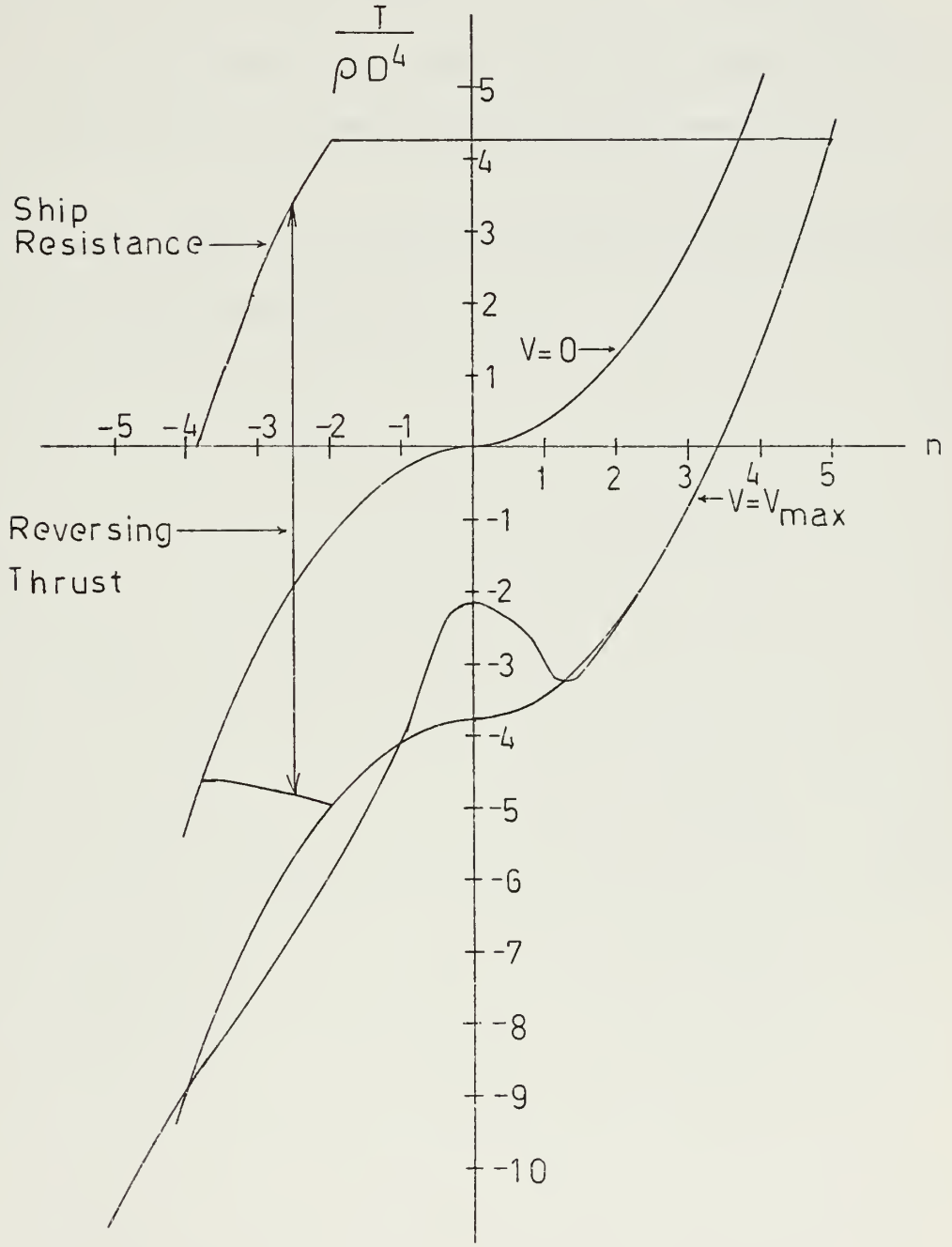

case throughout the ship speed transient. For the starting transient, thrust available is much less.

With a geared turbine plant, the ship speed transient starts while shaft speed is still positive during crash astern. With lower ship speeds, ship resistance decreases and the thrust curve shifts upward as shown in Figure IV. The net result is that there is much less thrust available throughout the maneuver and, consequently, the stopping maneuver takes much longer.

This discussion points out directly the advantage of the superconducting electric drive, greater maneuverability.

CONTROL SYSTEM DEVELOPMENT

At this point, the response characteristics of the ship and propeller are well defined. The objective of the control system is to provide maximum acceleration and deceleration capabilities, it is necessary to understand the response limitations of the electric drive system, the prime mover, and power plant. These limitations will demonstrate what can actually be realized by the superconducting plant for the crash astern and stop to full ahead maneuvers. The control system must account for the various limitations and minimize their effects on the desired responses.

There are two types of prime movers and power plants available that are reasonable for this application of 35,000 horsepower per shaft in a destroyer. The following are listed for consideration:

1. Conventional steam boilers and turbine generators.
2. Gas turbine driven generators.

Gas Turbine Power Plant

At present, gas turbine plants have a faster response than conventional steam turbine plants. There is not the problem of a time lag for heat buildup. The fuel governor can open full in three seconds and the turbine can be maintained at its most efficient rpm while being taken from 10 percent power to 100 percent power in perhaps fifteen seconds. This provides a distinct maneuverability advantage over the steam plant.

For crash astern, the gas turbine must be prevented from overspeeding upon removal of the load. This can be done by a quick-closing valve or substitute load.

Conventional Steam Power Plant

This plant consists of steam boilers and main generator turbines. Slow boiler response is the primary limitation imposed by this plant.

Assuming a turbine idling state at 10 percent power prior to commencement of the stop to full ahead maneuver, the turbine governor may open full in three seconds. However, the boilers could not meet this steam demand. Therefore, there is a lag in power until rated steam flow can be maintained. This lag may be sixty seconds or more, even on the newer 1200 psi steam plants. The limitation to the power buildup is due to the slowness of the boiler's heating up. Improvements in boiler design and controls may shorten this lag, but presently the response is significantly slower than that of a gas turbine plant. However, the advantage of the electric motor drive is still gained. With its much smaller rotating inertia as compared with a steam turbine and reduction gears, the superconducting electric drive allows more rapid attainment of any rpm. Hence, maneuverability is still improved over geared turbine plants.

For crash astern, the electric drive allows immediate removal of the load from the propulsion generator and application of dynamic braking. This may have grave consequences for the propulsion turbine and generator unless they can be slowed as soon as the load is removed, or another load is provided them. Closing a quick-acting valve automatically upon execution of crash astern is considered unacceptable since it would result in lifting boiler safety valves and lowering the water level in the boiler when, due to the effectiveness of dynamic braking, high steam rates would soon be required to drive the propellers into the negative rpm region. Also, there are other

operational situations where sharp reductions in power will be required. Use of a quick-closing valve may cause boiler safeties to lift on these occasions. Since safety valves must be checked and reset after every lifting, this is unacceptable as a regular occurrence.

The solution then seems to be the application of a substitute variable load resistor to the generator terminals. This resistor and its use are discussed later in this section.

It is seen that both the gas turbine and steam plants have definite rate limitations on changes in power. It remains to be seen how these limitations will affect ship response.

Any decision for the use of either plant would have to consider the above limitations with regard to specific mission requirements on a cost effective basis.

Electric Machinery

With constant rotor excitation at rated speed the synchronous generator does not produce full power until it reaches rated current output. It is limited directly by its prime mover in its response to increasing power demands.

For the stop to full ahead transient there are no response limitations on the synchronous motor. Constant maximum torque can be produced immediately, assuming rated current is available, since the motor will be in synchronism from $n = 0$. Again, due to prime mover limitations rated current may not be sustainable immediately.

In crash astern, the amount of reversing torque available is somewhat limited by the internal stator reactance. This effect is much less in a superconducting machine than in a conventional machine since the reactance is so small. The difference can be shown by use of an equivalent circuit and phasor diagrams. As noted in [11], neglecting stator resistance is valid for large machines such as this. It is assumed valid also for superconducting machines. Figure X shows the equivalent circuit for one phase of a balanced three phase synchronous machine. For dynamic braking, the

Figure X

Equivalent circuit of a synchronous machine connected to dynamic braking resistor. Generator operation.

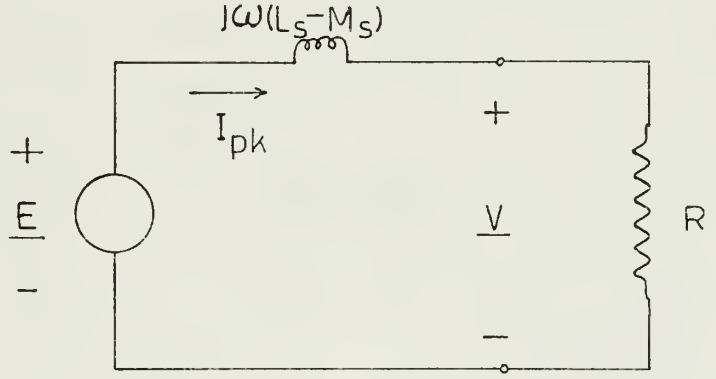

motor is connected to a fixed load resistor. From [11], Figure 6-5,

$$\underline{E} = \frac{L_{sr}\ \omega\ I_f}{\sqrt{2}}\ e^{j(\frac{\pi}{2} - \alpha)} \tag{13}$$

$$\phi = \tan^{-1} \frac{\omega[L_s - M_s]}{R} = \frac{\pi}{2} - \alpha \tag{14}$$

From Figure X,

$$\underline{V} = \underline{E} - j\omega\,(L_s - M_s)\,I_{pk} = I_{pk}\,R \tag{15}$$

Equation (15) defines the phasor relationships for Figure XI. For consideration of a two-pole machine, it is remembered that the total electromagnetic torque is given by

$$Q_e = -\frac{3}{2}\,I_f\,I_{pk}\,L_{sr}\sin\alpha \tag{16}$$

The constraints imposed in Figure XI are that I and $\underline{V}$ are constant. It is seen that if the rated reactance, L_s, for the superconducting machine

Figure XI

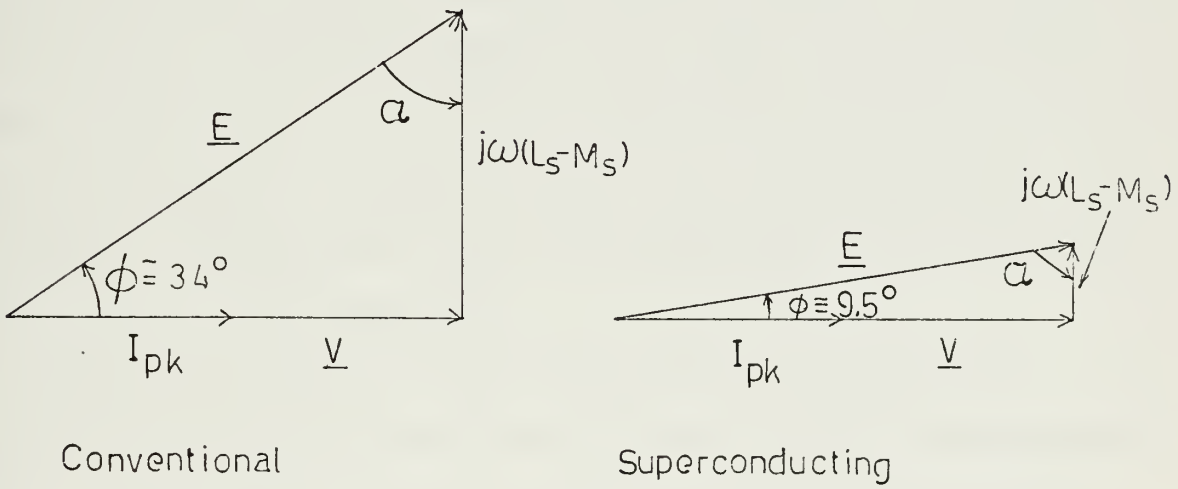

in this case is one-fourth that of the conventional machine, the ratio of the torques goes as

$$\frac{\sin\alpha_1}{\sin\alpha_2} \approx 1.18.$$

Another way of interpreting this is that this conventional machine produces only 84 percent rated torque in reverse while the superconducting machine produces nearly 99 percent. Of course, one could get higher torque from a much larger conventional machine. This indicates another prime advantage of the superconducting machine, size and weight reduction.

Control System - Gas Turbine Prime Mover

After listing and discussing limitations on performance, a control system is proposed that attempts to minimize their effects on desired ship performance as defined in the transient plots for an ideal system. A block diagram of this control system is shown in Figure XII. Response limitation of the gas turbine is handled by bridge control over the governor and voltage control. Bridge can control the point to which the governor opens. This control is tied to the voltage control in that the voltage control limits the rate of power application to the motor and the final value of armature current. In other words, this controls ship acceleration and final speed. Rate of power application is controlled to prevent stalling of the prime mover.

For any governor rate of opening there will be a particular time required for the gas turbine prime mover to come up to the commanded power level. The key factor of performance for a destroyer is maneuverability and fast response. Therefore, one would want the governor to open and close at a maximum rate to the desired setting. The ship acceleration or deceleration desired would determine initial governor setting. Final speed desired determines final governor setting. These settings are to be manually controlled from the bridge so that ship operators can have full control over

Figure XII

Functional block diagram of control system and plant. Other half of plant is identical.

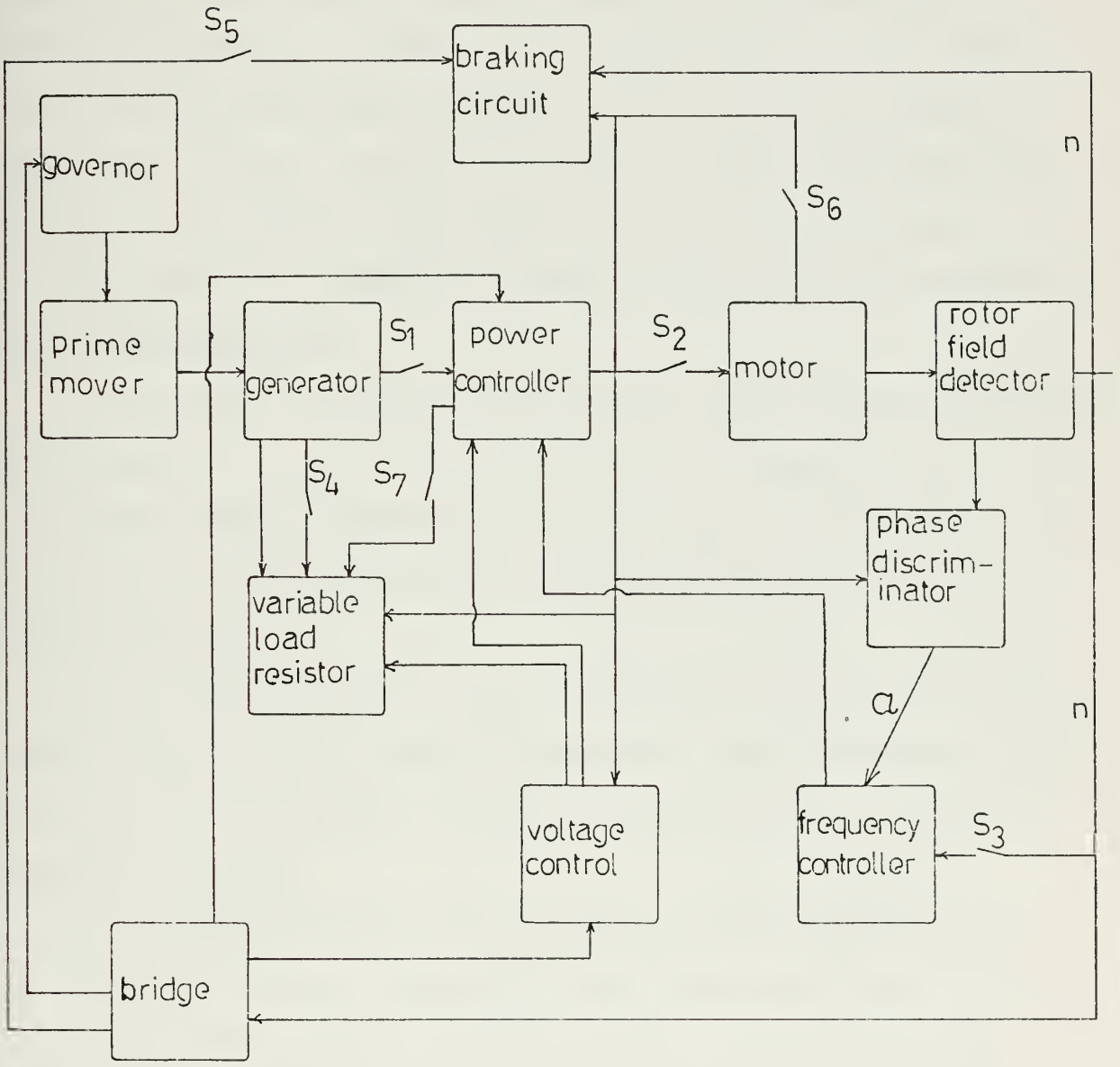

ship maneuverability. Operators would have the options of parallel plant operation and separate control of each plant. Cross connection of two generators on one motor would be possible, but at a reduced generator current level. One generator could also supply two motors.

A propulsion control station would be located in the gas turbine compartment. The station would serve to start the turbines and plant, control and monitor plant operation, and transfer control to the bridge. It would also be the secondary control station in the event of bridge remote control failure. In normal operation the bridge would control ship speed and, hence, propeller speed uniformly from zero to the maximum.

The entire electric plant would have standard ground fault protection.

Parallel Plant Operation

For this mode, the bridge would operate one control which simultaneously provides parallel control over the port and starboard plants. This would be the normal mode of bridge control. Separate control over the plants would be possible in situations where special maneuvering is desired.

Starting Maneuvers

With the bridge control in an off or stop position, the generators are idling at about 10 percent power at rated speed. Motor and generator field currents are at rated values. To start the ship transient, the following sequence takes place:

1. The governor is signalled to open to a particular power setting. Simultaneously, switches S_1 through S_3 close. The voltage control regulates motor power increase, current, and final values. Generator voltage and speed are constant. The frequency control, fed with the value of α,

regulates the frequency of the motor current through the power controller such that α approaches -90° and is held constant. This provides maximum available torque to the propeller shaft.

2. Motor torque is accelerating the propeller. The ship speed is essentially zero.

3. In a maximum of three seconds, the governor is open to its full setting. In a matter of perhaps fifteen seconds, the generator can provide full power. Motor torque will be limited to less than the maximum for part of this period because of the prime mover power limitation. Ship speed begins to increase.

4. Once any current setting is reached, motor torque is held constant while the ship and shaft accelerate toward their equilibrium operating point.

Acceleration

Each ship speed requires a certain steady state power. Maximum ship acceleration can be obtained to any speed by setting the governor to full open and, hence, the current setting to its maximum. Once desired ship speed is reached or approached, the governor can be reset and the voltage control ordered to reduce current in synchronism. It can be seen that any acceleration can be obtained in a similar manner.

Changing Speed

Increasing speed merely requires a higher governor and current setting corresponding to desired acceleration. When speed is reached, governor and current settings are reduced to their required steady state values.

Reducing speed requires reduced governor and current settings. Generator

load removal cannot be so fast as to overspeed the generator. Rapid load reduction or load removal requires use of a variable load resistor to prevent generator overspeeding.

Reversal - Crash Astern

To accomplish this maneuver, the following sequence takes place:

1. Switches S_1 through S_3 open while S_4 through S_6 close. This connects the braking circuit which varies motor load such that I_{pk} is maintained at rated value. S_4 connects the generator to the variable load resistor.

2. The braking circuit holds near maximum negative torque until the propeller reaches a particular positive n, which is determined by motor size and thermal capacity. At this point, switches S_4 through S_6 open while S_1 through S_3 and S_7 close. Phase sequence is changed and the motor is plugged and accelerated in the reverse direction.

The generator is capable of supplying rated current indefinitely to the motor since it is still at full power. The voltage control maintains rated current to the motor and varies the voltage. Slack in generator load is taken up by the variable load resistor. The resistance decreases as the motor draws more power.

3. The motor accelerates at maximum torque astern to a value of n corresponding to the ship speed. It is assumed that the ship has not decelerated significantly. From this point the ship decelerates.

4. At any speed, the bridge can stop the deceleration by reducing governor opening and current to the motor.

If at any time during the crash astern maneuver, when the motor is operating at a negative rps, it is desired to immediately accelerate ahead, a crash ahead maneuver following the above sequence is allowed by the control system.

Dynamic braking is considered necessary here since it is expected that the thermal mass of the motor will not be enough to absorb the energy involved in the maneuver. The hydrodynamic energy required to be absorbed by the motor during crash astern is calculated in Appendix B.

Control System - Conventional Steam Turbine

It is proposed that the same basic control system as shown in Figure XII applies equally well to this type of power plant. The significant difference is in the time required for the plant to come up to power. Also, rate of governor opening and closing must be limited so as not to lose steam pressure on stop to full ahead maneuvers or lift boiler safeties on slowing. General operation will be the same.

Starting Maneuvers

The sequence of events is the same as for the gas turbine. However, there is a time of perhaps sixty seconds required for the steam plant to increase power from 10 percent to 100 percent. This limits greatly the amount of torque available from the motor over a significant time period resulting in slower ship acceleration.

Acceleration and Changing Speed

As mentioned above, ship acceleration is much more limited by the steam plant's ability to increase power. Increasing speed is limited by the

acceleration obtainable. Decreasing speed is somewhat limited by the boiler's ability to decrease steam flow in correspondence with rapid load removal.

Reversal - Crash Astern

With dynamic braking, the steam turbine plant will provide exactly the same crash reversal characteristics as the gas turbine plant using this control system. The sequence of events for this maneuver is independent of the prime mover.

Control System Components

In this part of the report the various boxes, components of the control system, shown in Figure XII are discussed. These are discussed not to the point of an actual component design, but for the purpose of demonstrating their realizability and function in the control system.

Power and Frequency Controllers

These units, shown in Figure XIII, contain the silicon controlled rectifier, SCR, cycloconverter and firing logic circuits. Appendix B shows a simple three-phase cycloconverter and explains its operation. Since there is so high a power requirement, 26, 100 KVA per shaft, the SCR circuits have to be paralleled. At present, SCR's are available in the range of 1000 KVA rating.

The function of the power controller is to transmit power from the generator to the motor. It is fed constant frequency power from the generator. With the assistance of the frequency controller, variable frequency power is available to the motor. When using a full wave cycloconverter, the

Figure XIII

Power and Frequency Controllers.

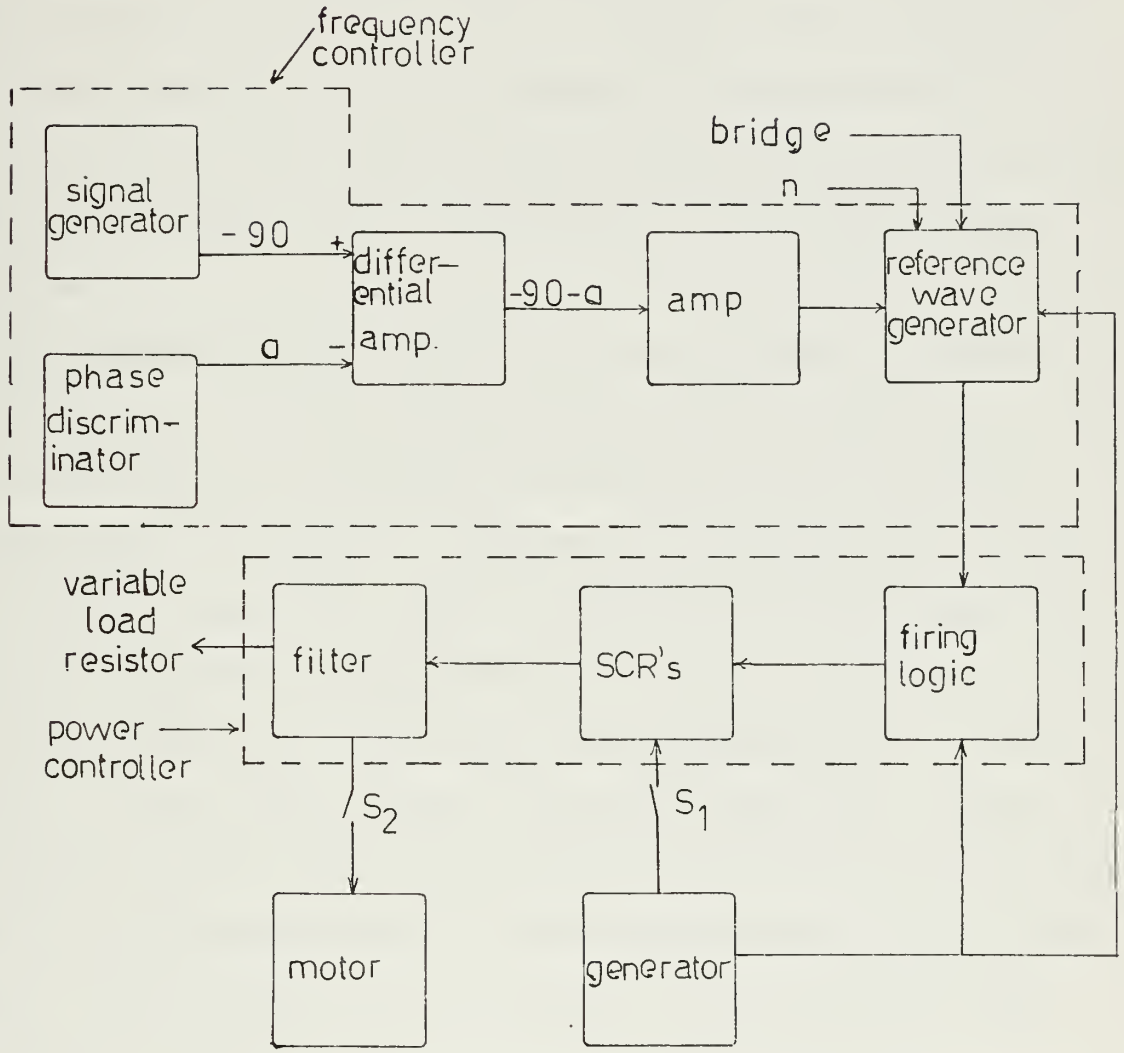

frequency ratio is at least two to one from generator to motor.

The frequency controller signals the firing logic circuits to adjust the firing angle on the SCR's of the cycloconverter, thereby changing output frequency. If α is greater than -90^{o}, the reference wave generator signals an increase in frequency. If α is less than -90^{o}, the reference wave generator signals a decrease in frequency. This maintains α at approximately -90^{o} at all times, the stator magnetic axis ahead of the rotor magnetic axis. Torque is then limited only by I_{pk} since I_{f} is at rated value always.

The frequency controller shown is just one possibility for maintaining proper phase relation between rotor and stator magnetic axes. Firing logic operation and reference wave generation can be similar to that described in [24] and [9]. Synchronism of the two propulsion motors is particularly simplified by using the same reference wave generator for both port and starboard control systems.

During dynamic braking these units are not connected to the motor and generator. However, when n reaches a particular ahead value, n_{o}, they are reconnected. The reference wave generator changes phase sequence which results in a corresponding change of phase sequence in the motor and motor reversal. The bridge may exercise independent control over motor phase sequence for $-n_{o} < n < n_{o}$.

Filtering removes the harmonic content of the power controller output and is discussed in [18] and [24]. SCR's would be provided with standard overcurrent protection devices.

Voltage Control

This unit functions to limit I_{pk} and control power application to the motor. In doing so, it controls motor torque, prevents motor overheating, and prevents prime mover overload.

The voltage control is programmed to allow power increase both at a rate in keeping with generator acceleration and to the governor and current setting commanded by the bridge.

As noted in [9] and developed in [2], the amplitude of the cycloconverter output voltage is also controlled by the reference wave generator. From [2], the equivalent circuit of Figure XIV is obtained.

Figure XIV

Equivalent Circuit of a Cycloconverter.

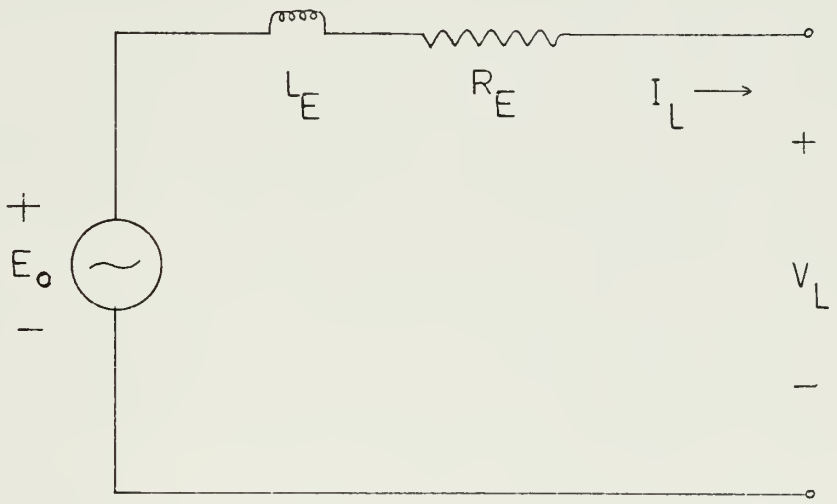

The source, E_o, is given by

$$E_o = K_1 E_{DO} \sin \omega_L t \qquad (17)$$

where ω_L is the reference wave frequency. K_1, ranging between zero and

unity, represents reference wave amplitude. E_{DO} is proportional to the peak amplitude of the phase supply voltage from the generator. This circuit is valid for most applications and particularly when the frequency ratio is five to one or more.

It is obvious then that basic to the control of applied voltage to the motor is the control of K_1. This is accomplished by the voltage control shown in Figure XV.

Referring to Figure XV, the block representing allowed rate of power change emits a ramp signal such as appears in Figure XIX. Its purpose is to limit the power applied to the motor to that capable of being produced by the prime mover and generator. The rate is assumed constant here and will be constant no matter the initial power level. The upper limit on power is set by the bridge.

Figure XV

Voltage Control

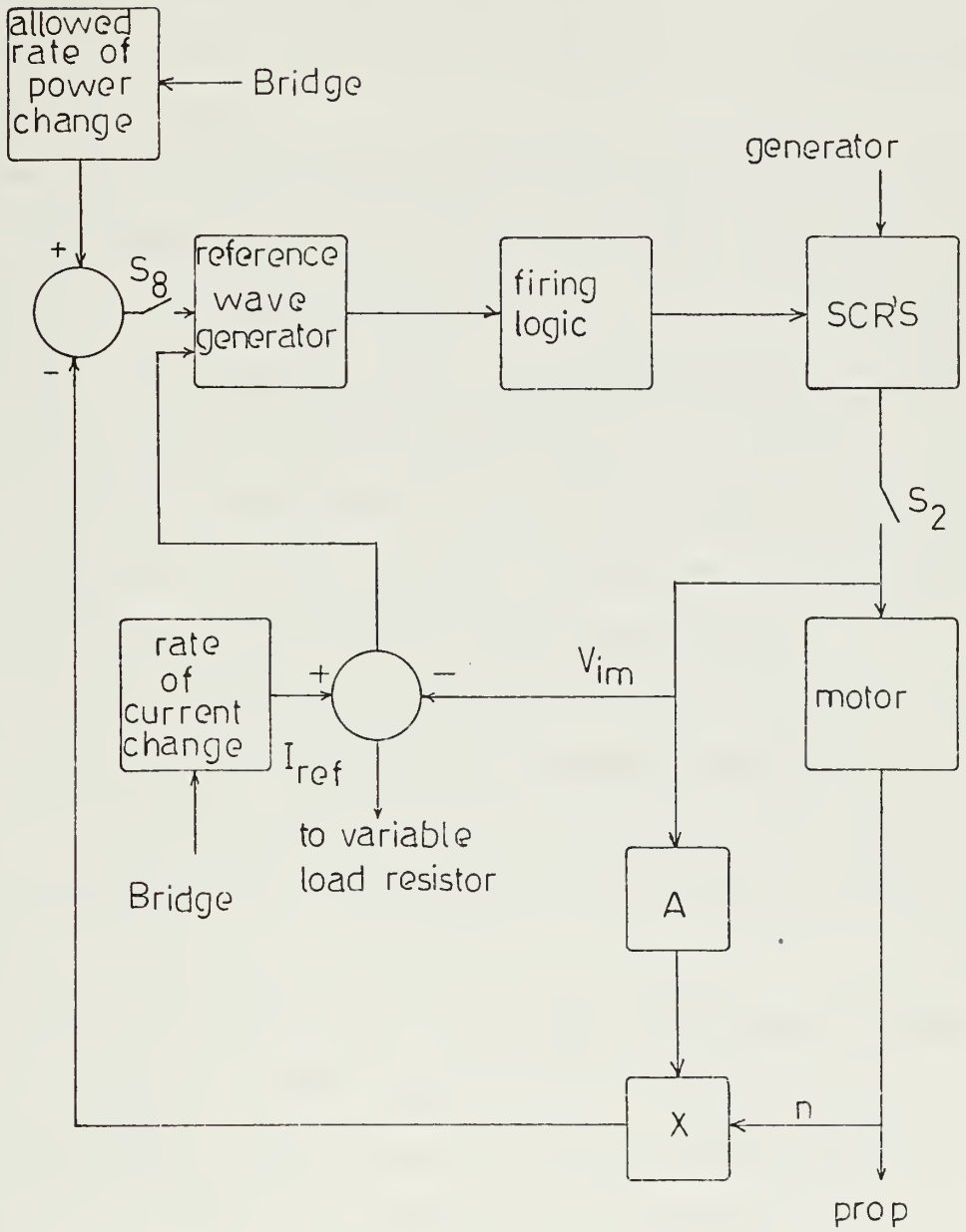

The rate signal is compared to a signal proportional to motor output power. The latter signal is obtained from the product of n and V_{im} times the appropriate constant. V_{im} is a voltage proportional to a motor phase current amplitude, I_{pk}. If the difference between the signals is positive, K_1 is increased. This increases the maximum allowed firing angle for the SCR's.

Another feature of the voltage control is a current limiter. This serves to limit motor current to that set by the bridge. The upper limit on current is the rated value. Any torque up to the maximum can be selected. On acceleration, the reference current is set instantaneously. It is compared with V_{im}. With a positive difference, K_1 is increased.

The reference wave amplitude, K_1, may then be thought of as regulated by two gain controls in series. One gain is influenced by the current limiter, while the other is influenced by the power limiter.

The reference wave generator by its amplitude tells the firing logic the maximum firing angle allowed. By its frequency, the reference wave generator tells the firing logic the frequency of firing for the SCR's. These are the same reference wave generator and firing logic shown in Figure XIII.

During dynamic braking, S_2 and S_8 are open. During motor plugging, S_8 remains open while S_2 is closed. I_{ref} is set at rated current so that maximum reverse torque is maintained. The signal to the variable load resistor tells it to absorb less power if V_{im} is less than I_{ref} and vice versa. This interplay is explained in greater detail when the variable load resistor is discussed.

For deceleration, other than crash astern, S_2 and S_8 are closed. Depending on maneuverability desired, there can be various rates of power and current decrease. During these decreases, it is assumed that the governor can maintain the prime mover at constant speed.

The rate of decrease signals could be decreasing ramps of various slopes. The maximum slope allowed would be that where the motor could no longer absorb propeller energy without overheating.

The voltage control could also have motor overspeed protection built in. If n exceeds its limiting value, the current reference signal would be cut off forcing K_1 to zero. The prime mover has its own overspeed protection. Motors and generators also have standard ground fault protection devices.

Excellent discussions of the use of SCR cycloconverters for variable speed A-C motor drive are contained in [9] and [18]. Both list many advantages of such control. SCR hardware built and tested for this purpose is pictured and discussed in [18]. From discussion in these and other references, it is obvious that these controllers are proven devices.

Braking Circuit

The braking circuit connects the dynamic braking resistor to the motor terminals. It provides for dissipation of propeller hydrodynamic energy at near maximum torque. The circuit maintains armature current at its rated value. The angle α is not controlled but is not expected to deviate much from -90°. This is due to the small armature internal reactance. Even if α were -75°, $\sin \alpha \tilde{=} -.966$. This would mean less than a 4% loss in torque. Criticality of the loss of torque in reversal would influence motor design.

Control of the effective resistance seen by each phase of the motor is the principle of operation for this circuit. Actual resistance connected

to each motor phase is a constant. Effective resistance control is accomplished by inserting SCR's and appropriate firing logic in series with each armature phase and braking resistor. By controlling the conduction period of the SCR's, the current passing through the SCR's is regulated. This presents an effective resistance to each motor terminal.

As shown in Figure X and by equation (13), the magnitude of motor voltage and current depend directly on n. Therefore, as n decreases during reversal, the SCR's must conduct for a longer time. This allows current to be maintained at its rated value for maximum torque. By neglecting reactance in Figure X, one can see the relationship clearly.

$$|\underline{V}| = \frac{L_{sr}\ \omega\ I_f}{\sqrt{2}}$$

If $R = G\ \frac{\omega}{\omega_{max}}$, current can be maintained constant at its rated value. A simple way of achieving this control is shown in Figure XVI (a). Figure XVI (b) shows how armature current and SCR conduction period may vary with n.

The input, n, to the circuit merely acts as a signal to disconnect the braking circuit at $n = n_o$. The bridge input connects the circuit to begin the maneuver. V_{ref} corresponds to the desired rated current level. If V_m is less than V_{ref}, the firing logic decreases β, lengthening the conduction period, equally in each phase. This allows V_m to increase since more of the current waveform passes through the SCR's.

By the appropriate choice of G, the constant resistance, current is regulated at its rated value. Appendix B discusses the resistance, G.

Figure XVI

(a) Braking Circuit
(b) Armature Current

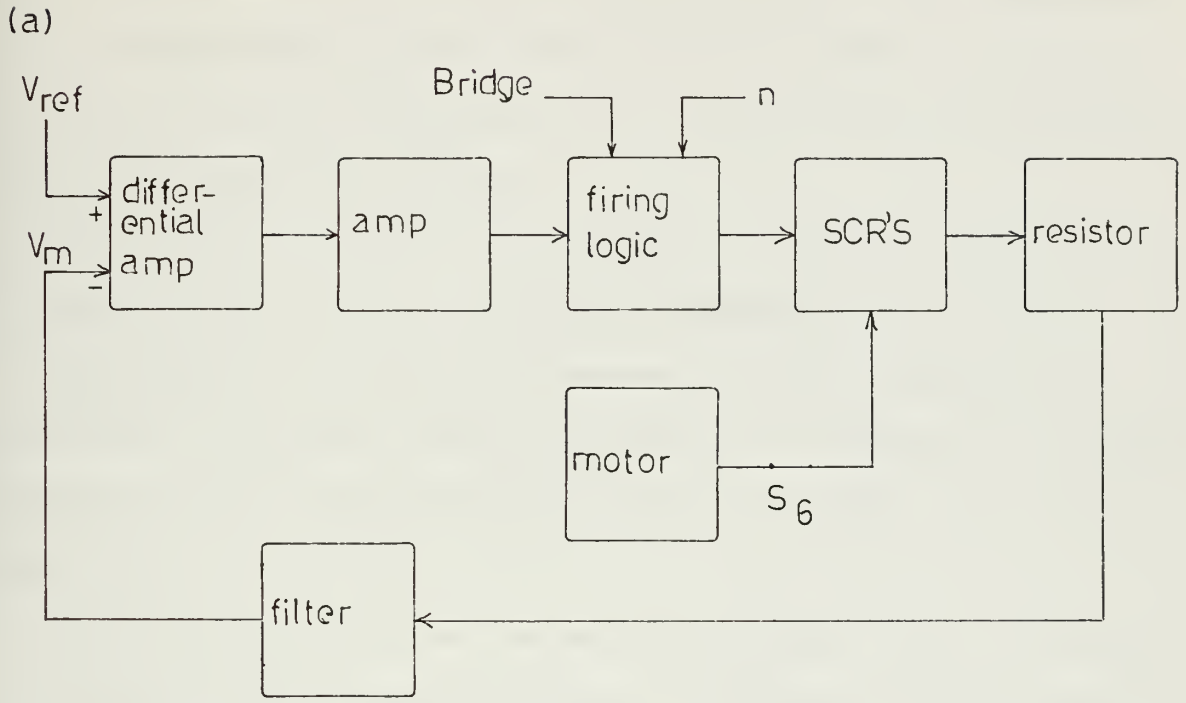

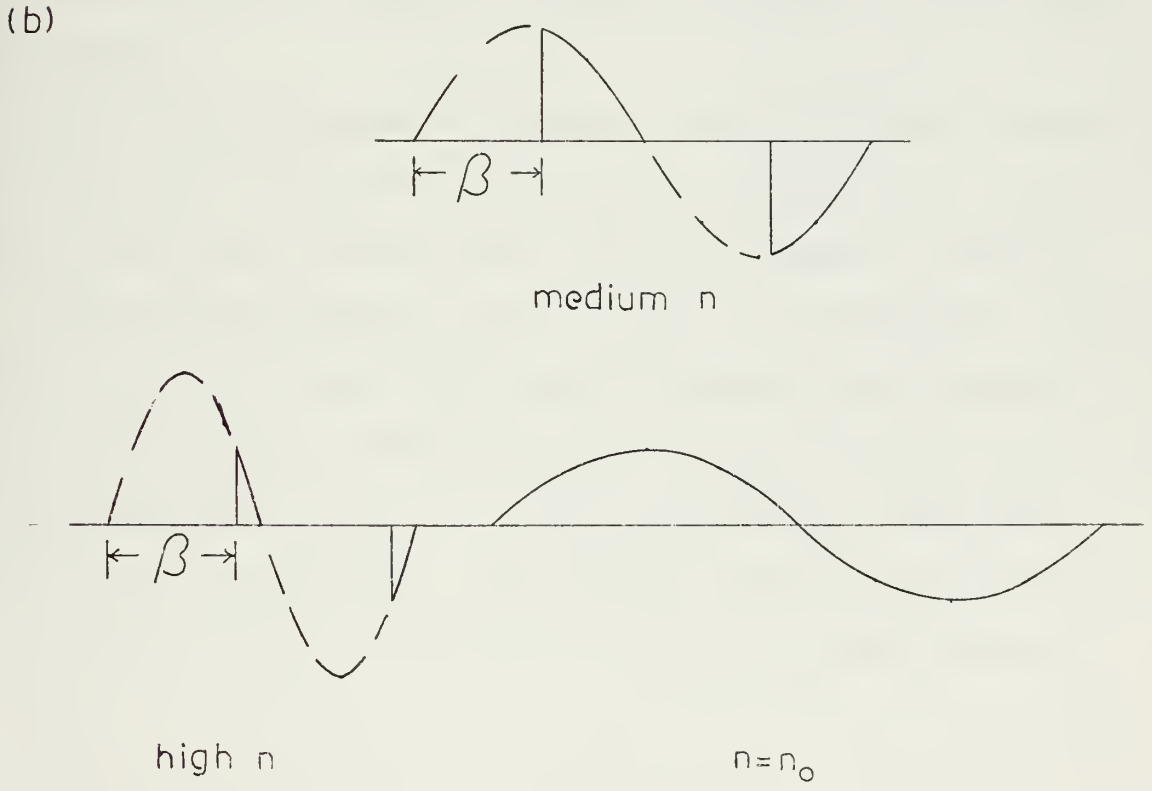

Generator Variable Load Resistor

During dynamic braking, a resistor loads each phase of the generator output at full power. This prevents generator and prime mover overspeeding. After the dynamic braking period, when the motor is plugged, the resistors must continue to load the generator, but at varying amounts, since the motor is not at full power for some time.

Inputs required for this device are some indication of power used by the motor and, then, how much power must be absorbed by the resistors.

During the entire crash astern maneuver, the motor is operating at rated current. Therefore, sensing the voltage at the terminals of one motor phase gives a direct indication of power used by the motor. This voltage signal is V_1.

The generator output is at constant rated voltage. Hence, if a signal, V_{ig}, is proportional to generator current, it indicates the power output of the generator.

Figure XVII is proposed as an example of how this device could operate. The resistor used here must be larger than that used for dynamic braking since it must absorb far more energy. This is discussed in Appendix B.

The difference between V_{ig} and V_1 is used as an instantaneous reference signal, V_{ref}. V_R is proportional to power absorbed by the resistor. If V_E is greater than zero, the firing logic is signalled to allow more current to pass through the resistor and dissipate more energy. The converse is true if V_E is less than zero. During dynamic braking, S_4 is closed while S_1, S_2, and S_7 are open. During ahead operations, S_4 and S_7 are open.

Figure XVII

Variable Load Resistor Device. Configuration: Motor Driving Astern.

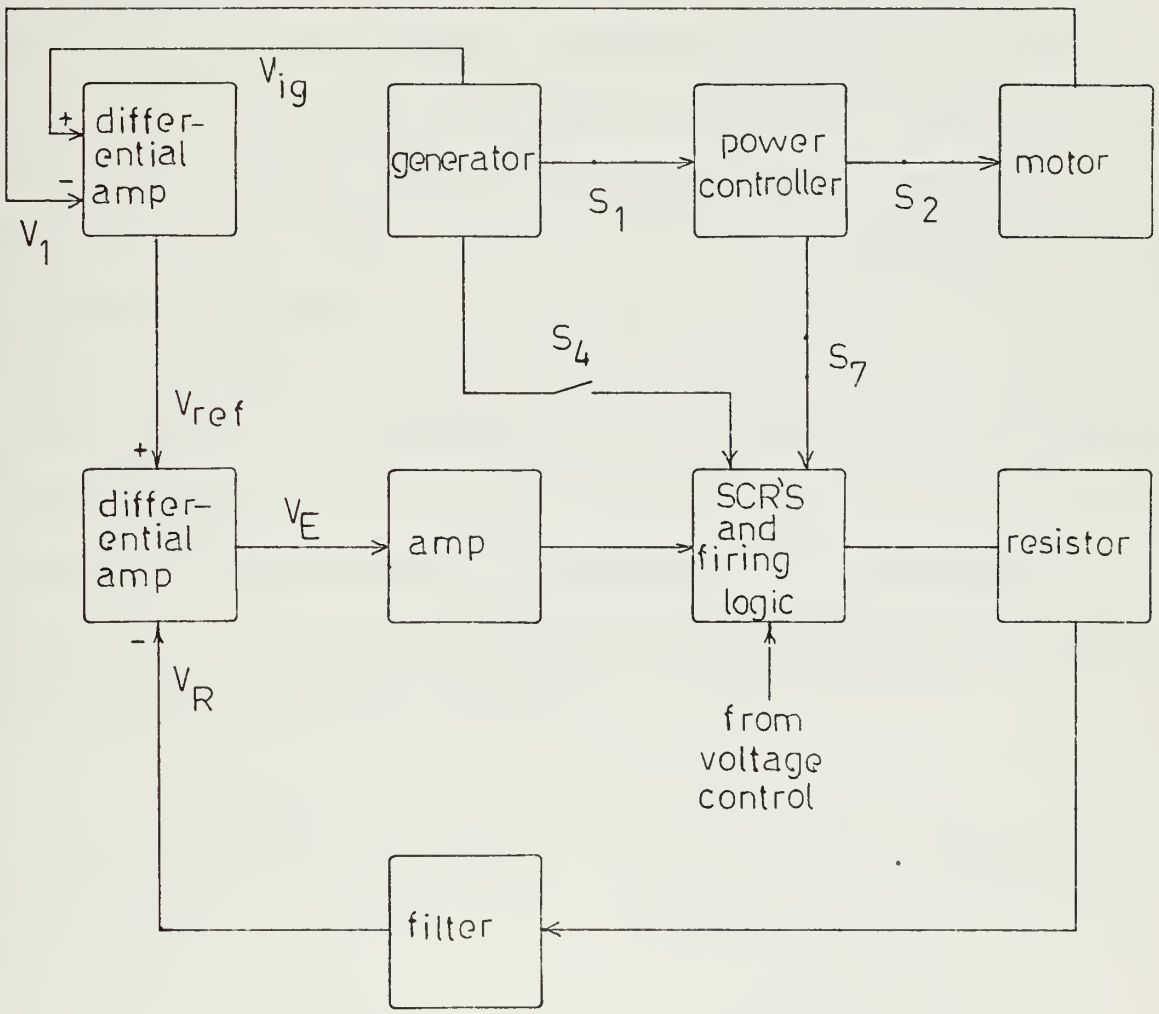

Since the voltage control, during motor operation, regulates the power output of the power controller, there needs to be an additional check to insure that rated current is maintained. In Figure XV, the voltage control signals for rated current, but this current is fed into a parallel load, the motor and variable load resistor. Therefore, by further regulating current flow into the variable load resistor as shown, it is insured that rated current is supplied to the motor. Firing logic in this device is simpler. There is no frequency changing, but merely a regulation on firing angle. This also insures that the generator is fully loaded down at full power.

Since crash astern is an emergency maneuver and is relatively fast, no attempt is made to reduce generator power level during the entire maneuver.

Rotor Field Detector

With a single phase winding, the rotor field axis is as shown in Figure XVIII (a). Figure XVIII (b) demonstrates the manner of sensing the angular position of the rotor field axis.

Figure XVIII (a)

Motor rotor configuration.

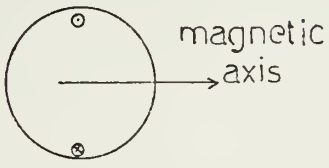

(a)

Figure XVIII (b)

Rotor magnetic field detection scheme.

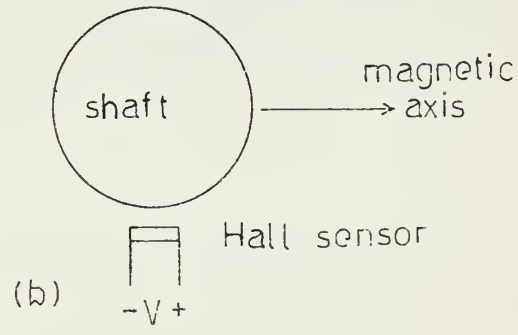

(b)

At some point along the propeller shaft, magnetic poles are attached so as to produce a sinusoidally distributed magnetic field about the periphery of the shaft with its maximum value along the rotor magnetic axis. Using a Hall Effect semiconductor sensor, a sinusoidal voltage is induced as the shaft rotates. This voltage is proportional to the current through the Hall device and to the instantaneous magnetic flux density seen by the device. The voltage will be of the same frequency as shaft rotation and armature current. As an input to the phase discriminator, the Hall voltage will differ in phase and magnitude from the armature current detection voltage.

Armature Current Detector

It is shown in Appendix B that one can sense a voltage that is directly proportional to an appropriate motor phase current which indicates the position of the armature magnetic field axis. The detector is a small precision resistor placed in series with the appropriate phase.

The phase relationship between the field detection voltages is also shown in Appendix B.

Phase Discriminator

The inputs to this device are the sinusoidal magnetic field detection voltages. Phase difference between the two signals is discerned by this device. This difference is fed into the frequency controller as shown in Figure XII and XIII. There are circuits available that will do this phase discrimination. Examples of such circuits are discussed in [6], [15], and [20].

RPS Detector

This device provides instantaneous indication of propeller shaft revolutions to the bridge, braking circuit, and frequency controller. Output

will be continuous from near zero to full rps. Examples of devices appropriate for use here are discussed in [12] and [23].

Bridge Controls

The essential bridge control would be the power control which sets governor opening and armature reference current. Various deceleration rates could be built into this control as mentioned earlier. All maneuvers other than crash astern are controlled by the power control. This control, being proportional to power, can be calibrated in terms of steady state ship speed and/or shaft rpm.

Crash astern control is separate and would affect the necessary switching described. At any point during crash astern, the operator could terminate the maneuver by signalling for less prime mover power and motor current. If a rapid change ahead is required, the crash ahead could be used as mentioned earlier.

Ship operators would have shaft revolution and ship speed indicators. The ship speed indication would be by a pitot log system. Inaccuracies of this system are noted in [5].

By using the indicators provided, navigational aids, and relative velocity to ships information, the operators can exercise control to slow or speed up the ship by use of the power control. For any maneuver, when pitot log, rpm indicator, or seaman's eye indicate the appropriate moment, the operator can signal for the steady state power required for his desired speed.

Refrigeration

Although not directly a part of the control system, refrigeration equipment plays a direct role in overall plant performance. Without

refrigeration, electric machinery performance is severely limited.

Refrigeration needs and availability are discussed in Appendix B.

REALISTIC SHIP PERFORMANCE CHARACTERISTICS

The equations of motion are the same as developed in the first part of this report. They are equations (2a) and (5).

Gas Turbine Plant

Stop to Full Ahead Transient

The initial conditions for this transient are that the plant is operating at the 10 percent power level with ship and shaft speed at zero. At t = 0, the governor is signalled to open full and reference current is set at rated value. The frequency controller adjusts motor armature excitation frequency keeping $\alpha = -90^{\circ}$. The voltage control prevents prime mover overload, motor overcurrent, and allows power input to the motor to increase accordingly with generator output power.

As mentioned earlier, the gas turbine power transient is assumed linear from 10 percent to full power. This is shown in Figure XIX. Also shown is the motor output power for the ideal transient. It is seen that with rated current applied steadily to the motor, the ideal motor output power surpasses turbine available power in approximately .8 seconds. In 11.4 seconds, the available power finally matches the motor output power.

In order to compute this transient, it is assumed that when the bridge orders the governor to open full and signals the voltage control to apply voltage to the motor, that rated voltage is applied. This is assumed enough to force motor current at zero rps to its rated value. Rated torque will then be applied immediately for a short duration and motor output power follows generator output power from t = 0 to $t \tilde{=} 11.4$ seconds.

Figure XIX

Power responses of practical gas turbine
and motor of ideal transient.

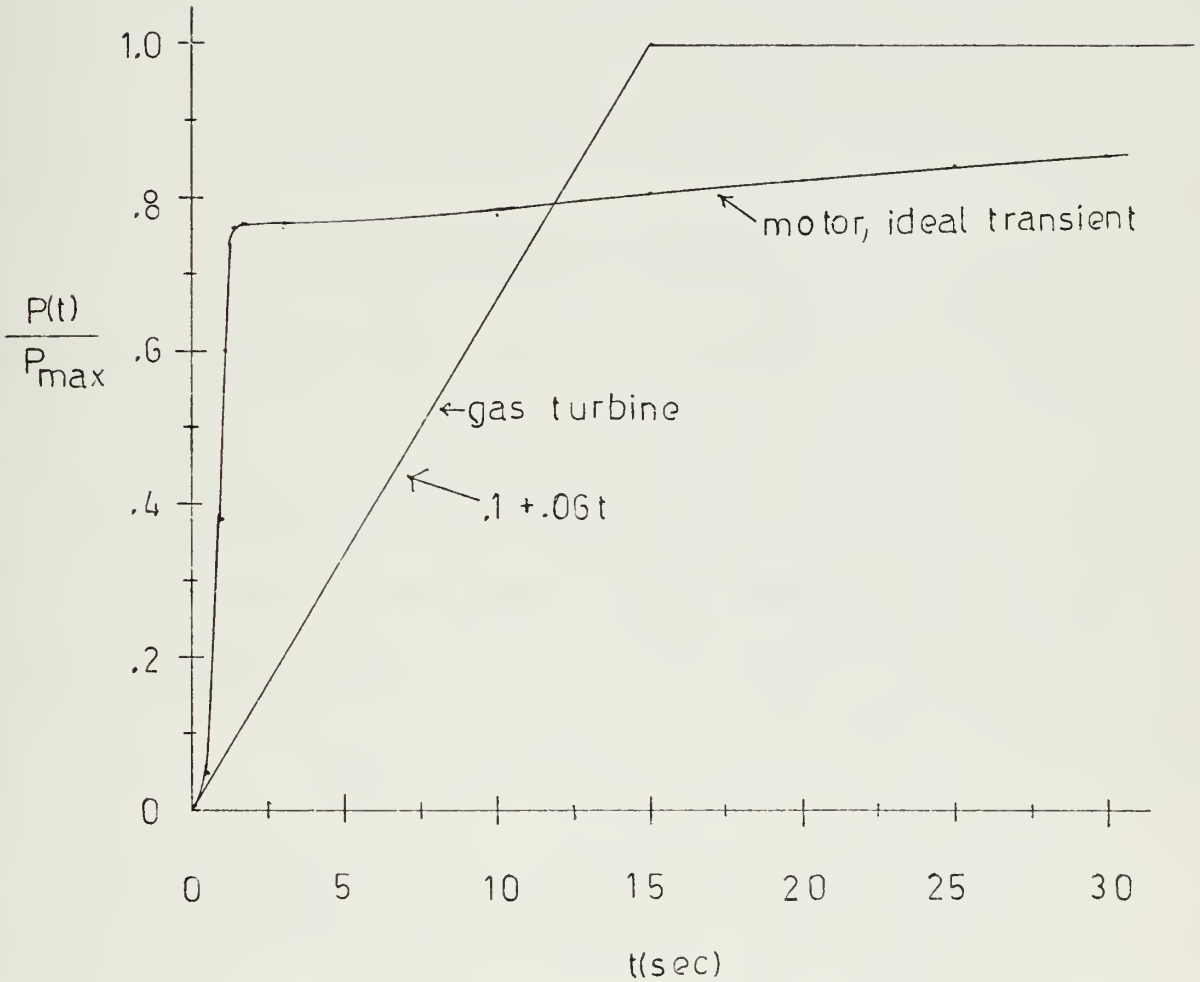

Shaft Transient

As before, it is assumed that v = 0 for the duration of the shaft transient. However, applied motor torque is not constant for this transient. Initially, motor electromagnetic torque is a maximum. This results in the exact response, initially, as for the ideal transient. Maximum torque is maintained until

$$\frac{P(t)}{2\pi n} = Q_{e\ max} \tag{18}$$

where,

$$\frac{P(t)}{2\pi} = 6.12 \times 10^{6}\ (.1 + .06t)$$

$$Q_{e\ max} = 1.224 \times 10^{6}\ \text{ft-lbs}$$

This results in equation (19).

$$n = .5 + .3t \tag{19}$$

Solving equations (7) and (19) simultaneously, one obtains a solution at n = .51 rps and t = .045 seconds. The next segment of the transient is governed by equation (20).

$$\frac{dn}{dt} = .93 \times 10^{-5} Q_e - .785\ n^2 \tag{20}$$

It is seen, however, that by evaluating the terms on the right hand side of (20) that the second term is less than 2 percent of the first. It will therefore be neglected in the solution for n until $\frac{dn}{dt} = 0$. Initially, this is a good approximation for the solution of n. Proceeding with the

solution,

$$\frac{dn}{dt} = \frac{57}{n} (.1 + .06t) \tag{20a}$$

By standard integration technique,

$$n^2 = 11.4t + 3.42t^2 - .255 \tag{20b}$$

When t = .36 seconds, $\frac{dn}{dt} = 0$, and n = 2.07 rps.

At this point, with v = 0, $\frac{dn}{dt} = 0$, and equation (21) applies. Solution for n is found by equation (21a).

$$.785\, n^2 = .93 \times 10^{-5}\, Q_e = \frac{57}{n} (.1 + .06t) \tag{21}$$

$$n = 4.17\, [.1 + .06t]^{1/3} \tag{21a}$$

At t = 11.0 seconds, n = 3.8 rps. With v = 0, this is the point in Figure III corresponding to maximum propeller torque and 76 percent rated power. This is the same power point in Figure XIX at t = 11.0 seconds. From this time, the motor is producing rated torque. The ship begins to increase speed and equation (5) becomes

$$n^2 = \frac{.93 \times 10^{-5}\, Q_e + 3.29 \times 10^{-3}\, v^2}{.785} \tag{22}$$

Ship Speed Transient

This transient is governed by equation (2a). Substituting for n^2 from (22), one obtains equation (23).

$$\frac{dv}{dt} = -.727 \times 10^{-3}\, v^2 + .15 \times 10^{-5}\, Q_e \tag{23}$$

With $Q_e = Q_{e\ max}$, equation (23) becomes equation (9).

$$\frac{dv}{dt} = -.727 \times 10^{-3} v^2 + 1.83 \qquad (9)$$

Therefore, the ship speed transient is the same as that plotted in Figure V, but shifted by approximately 9.7 seconds.

The entire ahead transient is plotted in Figure XX. The results shown are slightly distorted in that n increases more rapidly than it actually would by a few seconds. This is due to the neglecting of the second term on the right of equation (20) in the solution for n. Also, the ship speed will differ from zero within eleven seconds. This difference can only be negligibly small. In general, it is felt that Figure XX portrays the nature of performance that can be expected with a gas turbine prime mover, the control system described, and the superconducting electric drive.

Conventional Steam Plant

Stop to Full Ahead Transient

The initial conditions are the same as for the gas turbine maneuver. At t = 0, the steam turbine governor is signalled to open at a rate in keeping with the plant's capability to increase power. The plant capability is dependent on its control system and design. Here it is assumed that the steam plant can increase power from 10 percent to full in 60 seconds. The voltage control is signalled to allow the motor to be excited with all available power while limiting current again so that its rated value is not exceeded. Power available to the motor is shown in Figure XXI.

Figure XX

Stop to full ahead transient with practical gas turbine.

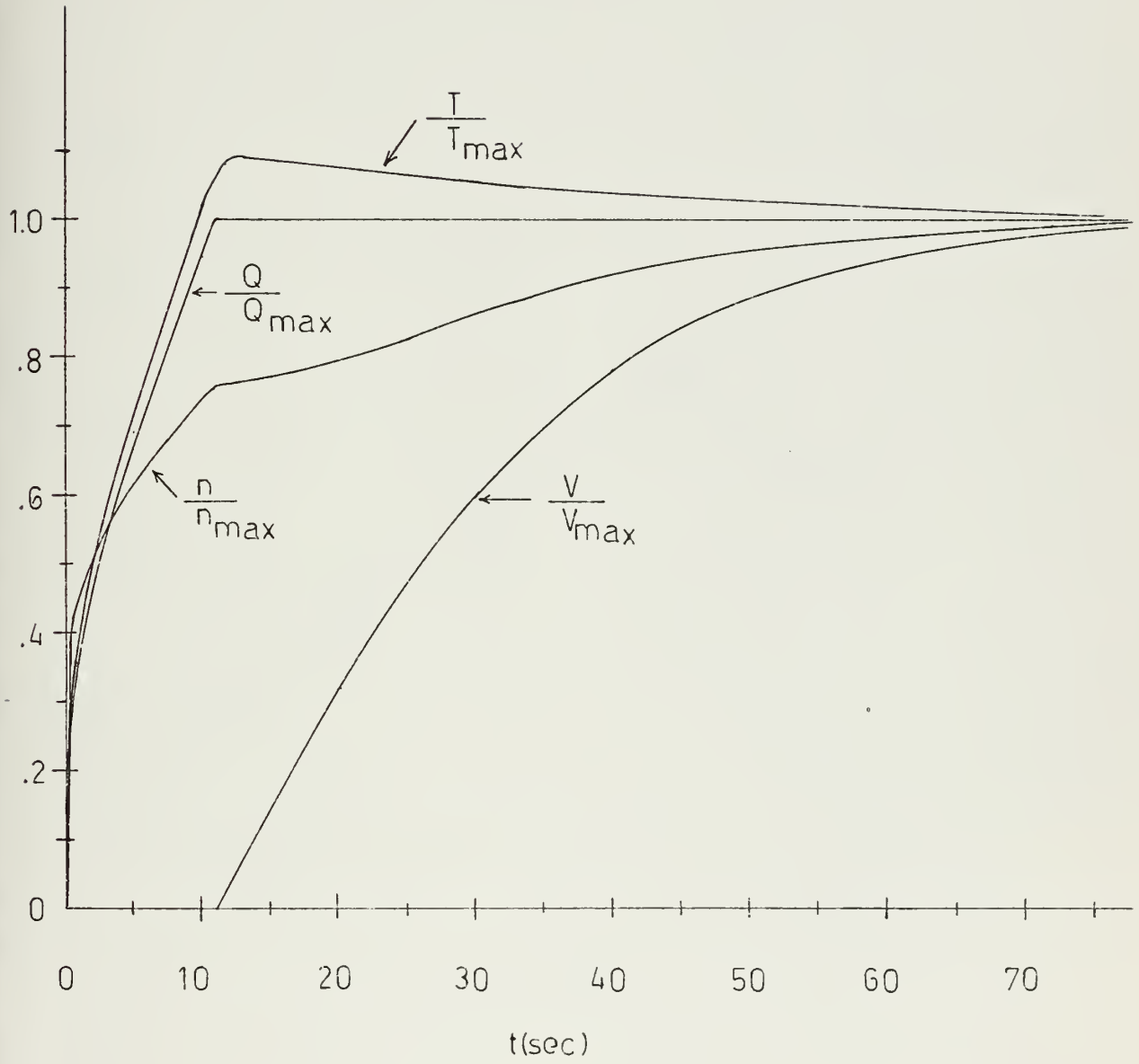

Figure XXI

Power response of conventional
destroyer steam plant.

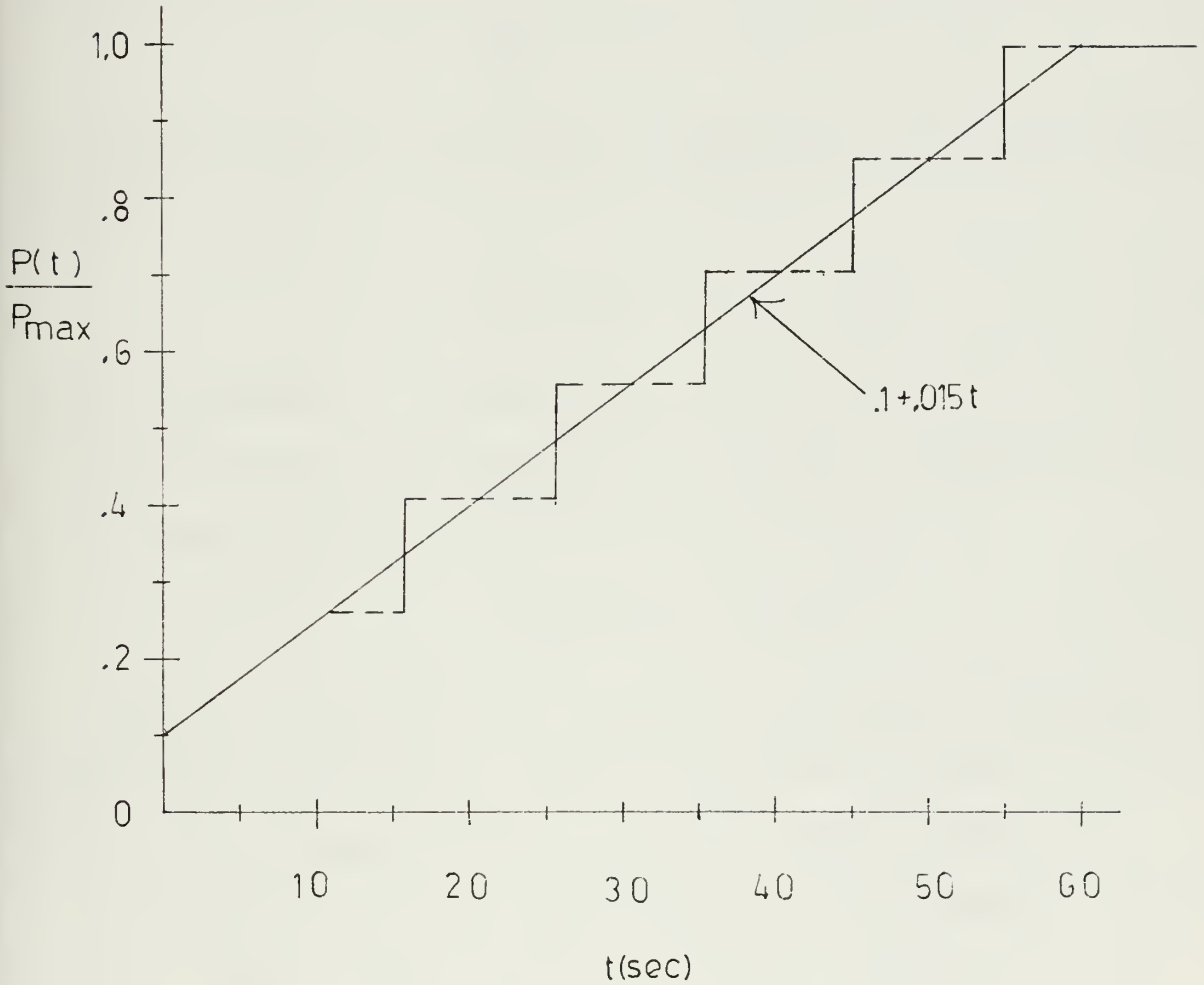

Shaft Transient

With maximum torque applied immediately, the shaft increases speed to $n = .503$ at $t = .04$ seconds as shown by solution of equation (18) for equation (24) and the simultaneous solution of (24) and (7).

$$n = .5 + .075t \tag{24}$$

The next segment of the transient is solved from equation (20) as for the gas turbine. Neglecting the second term again, one obtains

$$\frac{dn}{dt} = \frac{57}{n} (.1 + .015t) \tag{25}$$

By separating variables and integrating equation (25), one obtains equation (26).

$$n^2 = 11.4t + .856\ t^2 - .204 \tag{26}$$

At $t \approx .35$ seconds, $n = 1.97$ rps and $\frac{dn}{dt} = 0$. This is just over 4 rpm less than the gas turbine plant had achieved at this time. Modifying equation (21) for the next segment of the transient, one obtains

$$n = 4.17\ (.1 + .015t)^{1/3} \tag{27}$$

Solving (27) results in $n = 3.8$ at $t = 43.5$ seconds; the propeller is absorbing maximum torque. However, it is unreal to assume $v = 0$ this long. Let it be assumed, then, that v begins increasing from zero at $t = 11.0$ seconds and $n = 2.68$ rps. Power level is 26.5 percent. Ship speed could not increase sooner than for a gas turbine because of the great torque and power level differences. However, since with the gas turbine plant, the ship started moving at $t = 11.0$ seconds, it is assumed to be the best that the steam plant could do for this comparison.

Ship Speed Transient

The equations of motion for this transient now become (22) and (23). Substituting for Q_e in (23) gives

$$\frac{dv}{dt} = -.727 \times 10^{-3} v^2 + \frac{9.18}{n}(.1 + .015t) \qquad (23a)$$

To solve this equation, the second term on the right is approximated as a constant over equal time intervals as shown in Figure XXI. This is done for ease of computation. Areas under the curves are equal. Integrating equation (23a), one obtains

$$\int_{t_1}^{t_2} dt = 1375 \int_{v_1}^{v_2} \frac{dv}{S - v^2} \qquad (23b)$$

where S is a function of n and t. Initially, S = 1250 as shown by equation (23c). In (23c),

$$S = 1375 \left(\frac{9.18}{n}\right) (.1 + .015t) \qquad (23c)$$

n is the value of rps existing at the beginning of any of the equal time intervals; t is that time where the midpoint of the interval intersects the linear power curve in Figure XXI. Sample calculations for this part of the ship speed transient are shown in Appendix A.

At t = 55.1 seconds, $v = .85\ v_{max}$ and n = 4.69 rps while propeller torque is approximately 99.2 percent of maximum. From this point it is assumed that the transient continues with maximum applied motor torque. Applicable equations again are (9) and (22). The results are shown in Figure XXII.

Figure XXII

Stop to full ahead transient with steam plant.

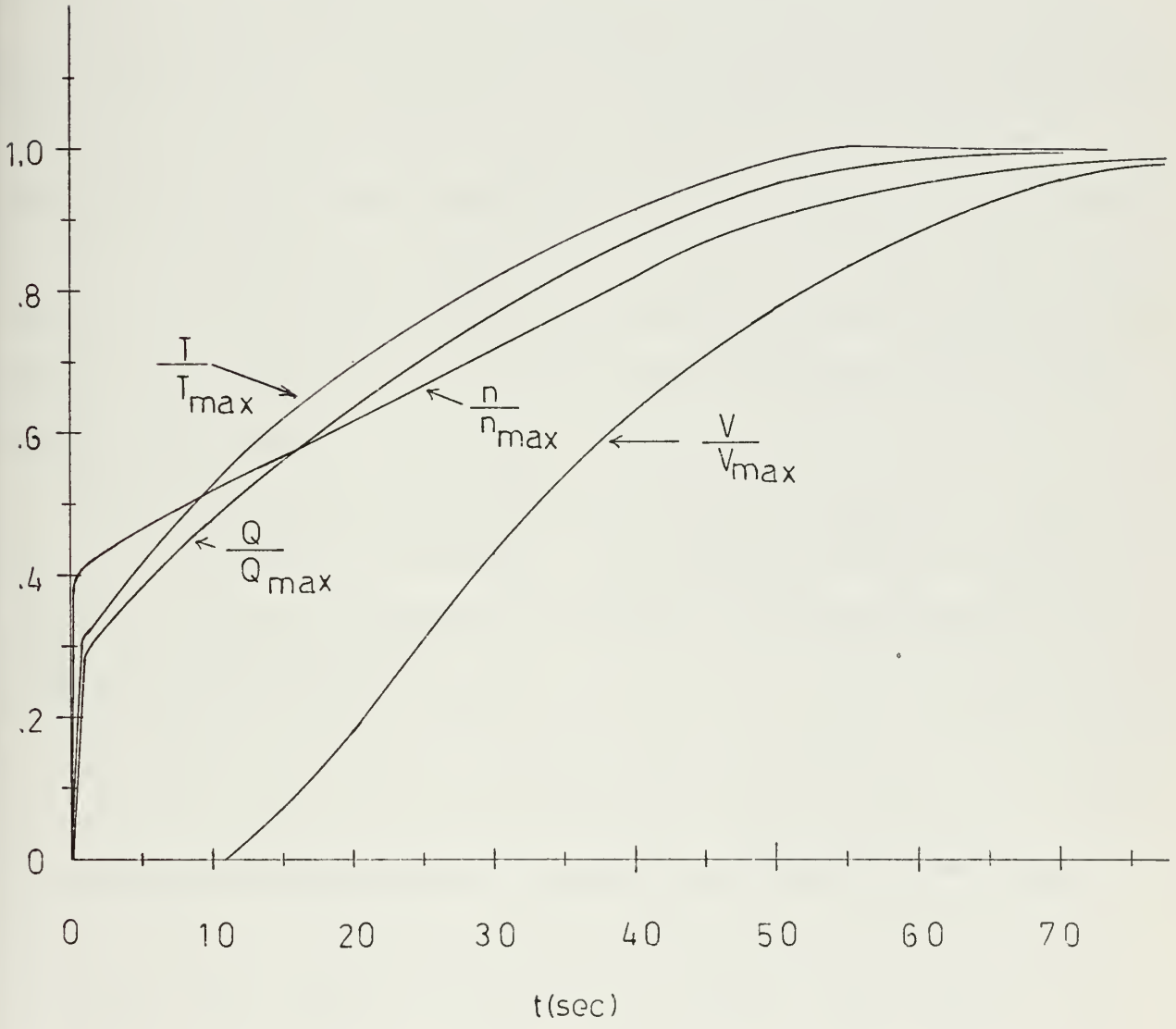

Crash Astern From Full Ahead

This transient with slight modification will be the same as the ideal for both gas turbine and steam prime movers. Again, the prime movers do not affect this transient because of the variable load resistor.

Immediately upon signal for crash astern, the generator load is shifted to the variable load resistor and the motor is loaded by the braking circuit. This requires no more than one second.

With an allowance for armature reactance of .2 per unit as maximum [8], motor reverse torque is 98 percent of the rated ahead value. The shafts are decelerated with this torque to n_o rps. The motor is then plugged and controlled to provide rated astern torque for the remainder of the transient.

It is assumed for this computation that $n_o = .25$, 15 rpm. Again, the actual value of n_o for any application depends on the thermal capacity of the motor and the limiting value of rpm below which the braking circuit cannot provide rated current.

Initial conditions for the transient are that $v = v_{max}$ and $n = n_{max}$. At $t = 0$, crash astern is signalled. It is assumed to require one second for motor torque to be reversed to 98 percent of rated ahead torque. The governing equation with $v = v_{max}$ is

$$\frac{dn}{dt} = -2.85 - .785\, n^2 \qquad (28)$$

By standard integration technique, equation (28) yields $t = .785$ seconds at $n = .25$ rps. At this point the motor is plugged and accelerated astern at rated torque. Between $n = .25$ and $n = 0$, equation (11a) applies. An

additional .08 seconds is required to reach n = 0. This assumes no lag due to switching.

From this point, the equations of motion are the same as for the ideal transient. It again requires an additional 2.14 seconds to reach n = -1.98 rps. Ship Speed now begins to decrease and $\frac{dn}{dt} = 0$. Equations (12) and (12a) apply.

Figure XXIII displays the transient. It differs from the ideal by little more than one second total time. This is due mainly to the time required to reverse torque from full ahead. The reactance limitation to torque during dynamic braking had only a minor effect.

Figure XXIII

Practical Crash Astern Transient.

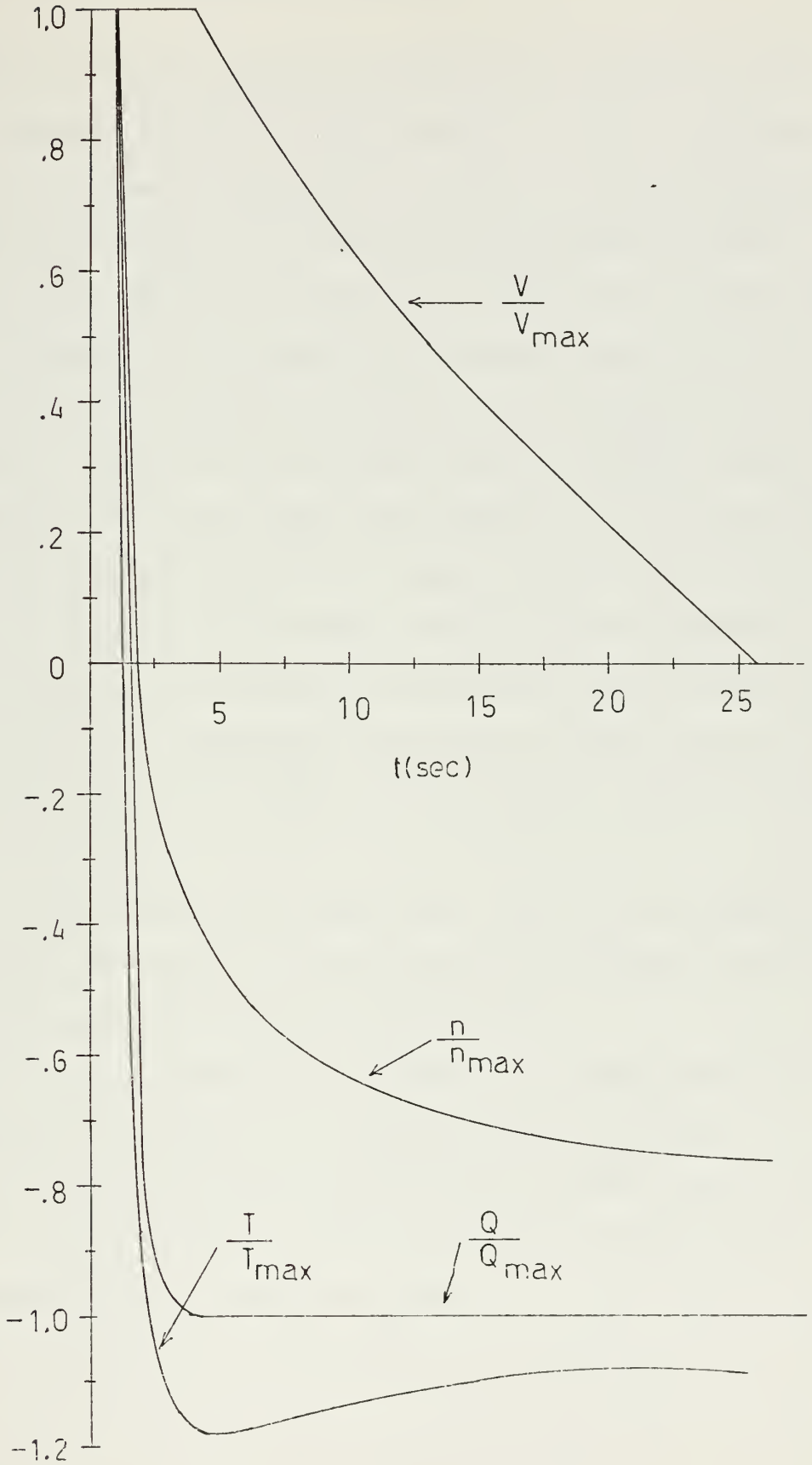

DISCUSSION OF RESULTS

The principal results shown in Figures XX, XXII, and XXIII are not intended to represent accurately the performance of a 3700 ton destroyer. They are merely intended to demonstrate the nature of expected performance in ideal weather conditions. The accuracy of the mathematical model is such that one could expect these results to be demonstrative of that nature.

Ship performance is not limited by the control system, but by the prime mover. The control electronics respond so fast that they are in the steady state with respect to the mechanical governors and prime movers.

With regard to the stop to full ahead transients, it is felt that the results for the steam plant system are perhaps a little better than can be expected. To approach these results, the plant must be poised for a rapid power increase. The ship speed transient would most likely be longer than shown since it was assumed here that it started at the same time as that for the gas turbine plant which itself responds in one-fourth the time.

Since the gas turbine plant responds much faster, the approximations made in computing that stop to full ahead transient are better justified. Hence, those results would also be less approximate.

The results for the crash astern transient are somewhat phenomenal. However, they are logical when it is remembered that total energy to be dissipated in stopping the shaft is so small that the shaft can be reversed very rapidly to provide much more astern thrust over the whole transient than is available with any conventional plant.

Reversing is also enhanced by the small synchronous reactance of the motor. This allows more reversing torque through dynamic braking than is available with conventional electric drives.

CONCLUSIONS

The conclusions are:

1. With the superconducting machines and the control system proposed, the crash astern characteristic is significantly improved over any other type of conventional drive system. The prime mover does not influence performance on this maneuver.

Actual trial crash astern transients for a 2315 ton destroyer of 50,000 shaft horsepower are pictured in [7]. From 32.8 knots, time required to stop the ship was 69 seconds. The ship had a conventional steam geared turbine drive. This trial cannot be compared directly to the ship considered here, but it certainly indicates the nature of crash astern transients obtainable with conventionally powered and controlled ships.

2. The results for the stop to full ahead maneuver are considered satisfactory and an improvement over presently attainable ship maneuverability.

3. The control system is not optimized by any means. The amount of switch gear and circuit breakers involved here may require too much space. These may also limit switching at high power levels.

There are three sets of SCR's in the control system. They are in the power controller, braking circuit, and variable load resistor device. It is felt that to decrease cost, the SCR's in the braking circuit could be used both for dynamic braking and loading the generator. The generator could be loaded by a fixed resistor during dynamic braking and then switched to the braking circuit when the motor is plugged.

4. The effect of actual ship resistance versus that assumed should be considered when evaluating the results shown.

RECOMMENDATIONS

The recommendations are:

1. As noted in [13] by Miniovich, Nordstrom's propellers have a low expanded area ratio, .45. By using a Miniovich propeller with a higher ratio appropriate for high speed ships, the results may be more completely representative.

2. The results are encouraging for this type of drive and control. They are worthy of further refinement by computer simulation. The control system, propeller characteristics, and ship resistance could be simulated on a digital computer as was done for an ice breaker in [10].

3. Research in high capacity refrigeration of liquid helium should be intensified.

4. A small superconducting machine of about 50 horsepower should be built which would be adaptive to various control methods. This would allow actual measures of performance to be made on the plant and controllers.

APPENDIX A

CALCULATIONS

Computation of Constants in Ship Motion Equation

From Figure I, with $v = v_{max}$ and $n = 5$, $\frac{T}{\rho D^4} = 4.26/sec^2$. This is for one propeller. Therefore,

$$T_t = 8.52 \rho D^4 = 52.2 \times 10^4 \text{ lbs}$$

It is recalled that

$$T_t(v,n) = -C_1(1-w)^2 v_{s\ max}^2 + D_1 n_{max}^2$$

or,

$$52.2 \times 10^4 = -C_1(2.52 \times 10^3) + 25D_1 \qquad (A1)$$

Also from Figure I, at idling speed, $T = 0$, $n = 3.42$ rps, and $v = v_{max}$. Therefore,

$$-C_1(1-w)^2 v_{s\ max}^2 + (3.42)^2 D_1 = 0$$

and,

$$C_1 = 4.67 \times 10^{-3} D_1 \qquad (A2)$$

Combining equations (A1) and (A2) results in

$$C_1 = 183 \frac{\text{lb sec}^2}{\text{ft}^2} \quad ; \quad D_1 = 3.925 \times 10^4 \frac{\text{lb sec}^2}{\text{rev}^2}$$

To evaluate K, equation (1a) is examined at maximum conditions in the steady state. This gives

$$0 = -(1-\mu)\ (1-w)^2 v_{s\ max}^2\ (183) + (1-\mu)\ \ 3.925 \times 10^4 n_{max}^2$$

$$-K(1-w)^2 v_{s\ max}^2$$

Solving this for K yields $K = 186 \frac{\text{lb sec}^2}{\text{ft}^2}$.

Computation of Constants in Shaft Motion Equation

At n = 5, v = 33 knots, $P = P_{max} = 70{,}000$ hp. Therefore,

$$Q_{e\ max} = \frac{70{,}000}{2\pi(5)} (550) = 12.24 \times 10^5 \text{ ft-lb}$$

From equation (4),

$$12.24 \times 10^5 = 25A - 2.52 \times 10^3 B \tag{A3}$$

To allow a closer fit of the model to the propeller characteristics, it was decided to let $\frac{Q_p}{\rho D^5} = -.55$ for each propeller at n = 0. Then,

$$-.55 = \frac{-B\ v_{max}^2}{2\ \rho\ D^5} \tag{A4}$$

or,

$$B = 354 \frac{\text{ft-lb sec}^2}{\text{ft}^2}$$

Substituting this in equation (A3) yields

$$A = \frac{12.24 \times 10^5 + 354\ (2.52 \times 10^3)}{25} = .845 \times 10^4 \frac{\text{ft-lb}}{(\text{rps})^2}$$

Computation of Propeller Moment of Inertia

From [16], propeller weight is given by

$$W = K\ D^3\ (MWR)\ (BTF) \text{ lbs}$$

D is expressed in inches. MWR is mean width ratio and is assumed to be .50 for a 4-bladed propeller. BTF is blade thickness fraction and is assumed to be .05. K is assumed as .26 for 4-bladed propellers. Substitution yields

$$M = \text{Mass} = \frac{W}{g} = 840 \ \frac{\text{lb sec}^2}{\text{ft}}$$

A radius of gyration is assumed at .21D. Then,

$$J = (.21D)^2 \ M = 6500 \ \text{ft-lb sec}^2$$

An allowance of 25 percent mass increase is allowed for the inertia of entrained water in the propeller. Total $J = 8125$ ft-lb sec^2.

Computation of Inertia of Motor Rotor

To compute the rotor inertia use will be made of optimizing equations relating power to geometry for a superconducting machine of this type. These equations were developed in [8]. A simple rotor structure is assumed as shown in Figure AI.

Figure AI

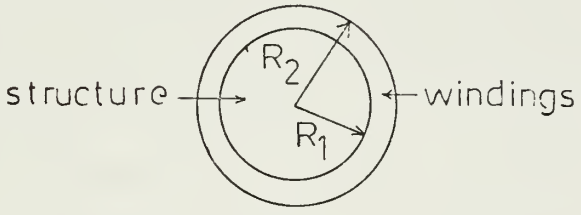

The applicable equations are:

$$P_m = \frac{6\mu_o \omega_m J_f J_a}{\pi^2} \ (1-y^{P+2})(x-\delta)^{P+2} \left(\frac{\ell_t}{R_o}\right) R_o^5 \left[\frac{1-x^{-P+2}}{4-P^2} + \frac{1-x^{P+2}}{(2+P)^2}\right] \qquad (A5)$$

$$\frac{\ell_t}{R_o} = \frac{\pi}{1.6}\,(1+x) \tag{A6}$$

$$x = R_{i/R_o} \; ; \; y = \frac{R_1}{R_2} \; ; \; \delta = \frac{R_i - R_2}{R_i} \tag{A7}$$

The symbols are listed below:

P_m - power

μ_o - magnetic permeability of space

ω_m - rotational angular velocity

J_f - rotor current density

J_a - armature current density

R_1 - rotor internal radius

R_2 - rotor external radius

R_i - armature internal radius

R_o - armature external radius

ℓ_t - length of rotor

P - number of pole pairs

The following values are assumed:

$y = .8$ $\qquad$ $J_f = 10^8 \frac{amp}{m^2}$

$x = .5$ $\qquad$ $J_a = 10^6 \frac{amp}{m^2}$

$\delta = .1$ $\qquad$ $P = 8$

Power factor is assumed to be .8. Values given are:

$$\omega_m = 10\ \pi\ \frac{\text{rad}}{\text{sec}}$$

$$\mu_o = 4\pi \times 10^{-7}\ \frac{\text{newtons}}{\text{amp}^2}$$

$$P_m = 2.61 \times 10^7 \text{ watts}$$

Substitution of all values in equations (A5), (A6) and (A7) yields:

$$R_o = .838 \text{ meters} = 2.75 \text{ ft.}$$

$$R_2 = .378 \text{ meters} = 1.24 \text{ ft.}$$

$$\ell_t = 2.46 \text{ meters} = 8.06 \text{ ft.}$$

Cylindrical solid geometry is assumed to compute an approximate value for the rotor inertia. The applicable equation is

$$J_m = 1/2\ m\ R_2^2$$

where m is rotor mass. Using the density for steel of 490 $\frac{\text{lb}}{\text{ft}^3}$,

$$m = \frac{490}{32.17}\ \pi\ R_2^2\ \ell_t$$

$$m = 594\ \frac{\text{lb-sec}^2}{\text{ft}}$$

Then,

$$J_m = \frac{594}{2}\ (1.24)^2 = 457 \text{ ft-lb sec}^2$$

This represents 5.62 percent of propeller inertia.

Sample Calculation, Steam Plant Stop to Full Ahead Maneuver

The purpose of this sample calculation is to illustrate the steps in solution of the steam plant stop to full ahead transient from t = 11.0 seconds. The governing equations are

$$\int_{t_1}^{t_2} dt = 1375 \int_{v_1}^{v_2} \frac{dv}{S-v^2} \qquad (23b)$$

$$S = 1375 \left(\frac{9.18}{n}\right) (.1 + .015t) \qquad (23c)$$

At t = 11.0 seconds, n = 2.68 rps and v = 0. The general solution for (23b) is $\Delta t = t_2 - t_1 = \frac{1375}{\sqrt{S}} \tanh^{-1} \left[\frac{v}{\sqrt{S}}\right]_{v_1}^{v_2}$. The first time interval, Δt, is 4.9 seconds and,

$$S = 1375 \left(\frac{9.18}{2.68}\right) [.1 + .015(11)] = 1250$$

Therefore,

$$\tanh^{-1} \left[\frac{v_2}{35.35}\right] = .1260$$

and,

$$v = .126 \ (35.35) = 4.45 \ \frac{ft}{sec}$$

Now equation (22) becomes

$$n^2 = 1.275 \left[3.29 \times 10^{-3} \ v^2 + \frac{57}{n} (.1 + .015t)\right] \qquad (22)$$

To solve for n, the following values are substituted in the right hand side of (22):

$$v = 4.45 \frac{ft}{sec}$$

$$n = 2.68 \text{ rps}$$

$$t = 15.9 \text{ sec}$$

This yields n = 3.05. However, iteration must be done to get a value of n that satisfies (22). Substituting again but with n = 3.05, yields the solution, n = 2.86. By iterating a few more times, one finds that n = 2.92 satisfies (22).

The next interval is from t = 15.9 to t = 25.7. For this interval,

$$S = 1375 \left(\frac{9.18}{2.92}\right) [.1 + .015 (20.8)] = 1778$$

With $\Delta t = 9.8$ seconds, v increases to 16.2 $\frac{ft}{sec}$, and iterating for n yields n = 3.39 rps.

This process is continued until t = 55.1 seconds. Then, n = 4.69 rps and $v = .85 v_{max}$. Also, $Q_P = .992 Q_{P\ max}$. The remainder of the transient is solved as in the gas turbine ship speed transient with maximum torque assumed.

APPENDIX B

SUPPLEMENTARY DISCUSSION

Three Phase Full Wave Cycloconverter

Figure BI is taken from [18]. It represents one of three identical phases of a three phase full wave cycloconverter.

Figure BI

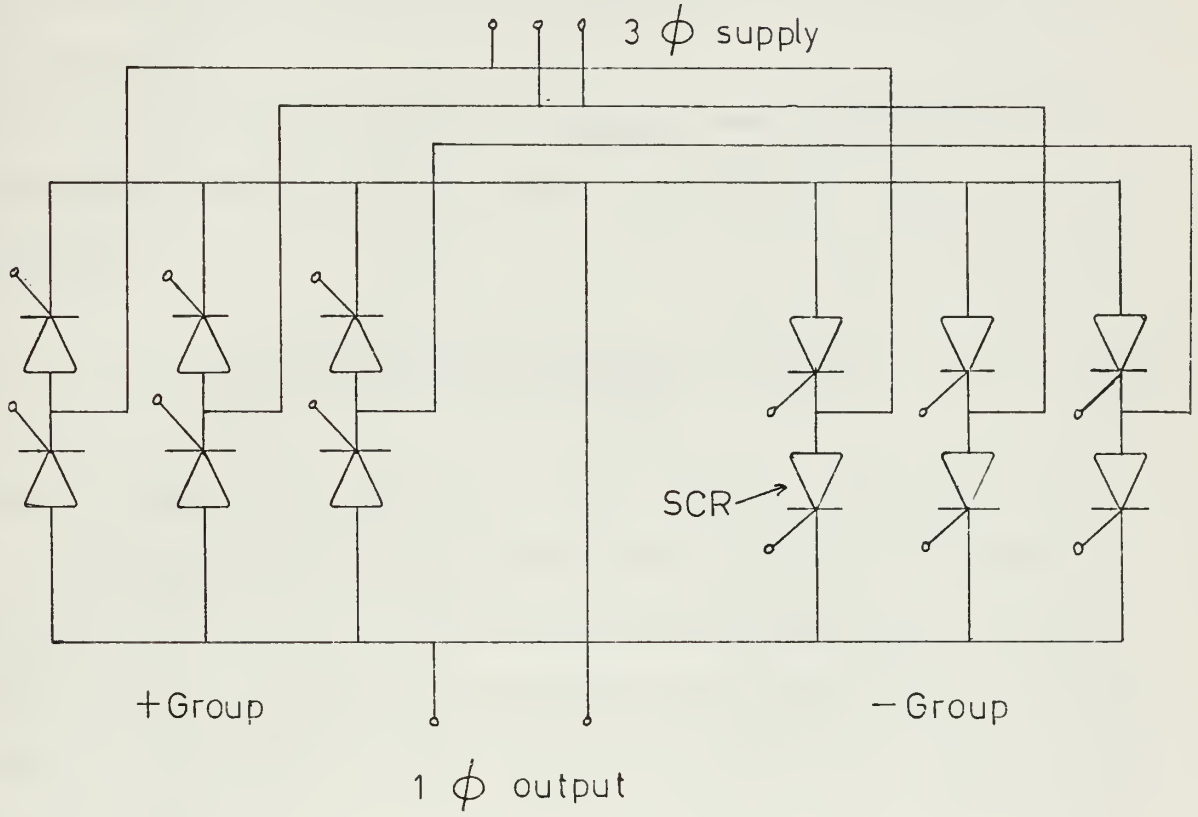

The positive group passes positive current to the load while the negative group passes negative current to the load. By selectively firing the SCR's in the positive or negative group, the load is provided with a controlled frequency signal of the desired polarity. Frequency is stepped down by 2 to 1 or more. This provides a wide range of motor (load) operation from a single generator frequency.

Several advantages of the full wave over the half wave configuration are listed in [18]. In addition, size, weight and pictures are shown for a

100 KVA frequency changer and logic module.

Braking Circuit Resistor, G

This resistor must absorb the hydrodynamic energy of the propeller in the crash astern maneuver. This energy is calculated later in this Appendix to be 10.4×10^6 joules. The result desired is the weight of the resistor required.

If the resistor were of copper with specific heat of .0918 $^{BTU}/_{lb\ ^oF}$, for a temperature rise of 100°C, the weight would have to be 50.6 lbs as shown below:

$$\frac{10.4 \times 10^6 \text{ joules}}{.0918 \frac{\text{BTU}}{\text{lb}^\circ\text{F}} \ (212\ ^\circ\text{F}) \ (1054.8) \frac{\text{joules}}{\text{BTU}}} = 50.6 \text{ lbs} \qquad \text{(B1)}$$

This represents total resistance for three phases. Each phase would have a 17 lb copper resistor connected for dynamic braking. The resistors could be cooled by sea water indirectly so that salt water stress corrosion cracking would not be a problem. The resistors themselves would be immersed in fresh water or some non-corrosive medium which would be surrounded and cooled by sea water.

The size of this resistor would certainly make it feasible for installation in a ship.

Variable Load Resistor

A rough idea of the size of this resistor is obtained by assuming that it must absorb full power for 2 seconds with a 100°C temperature rise. Proceeding as in equation (B1), full power for 2 seconds represents 104.4 $\times 10^6$ joules. The weight of the resistor is then about 510 lbs. This requires 170 lbs of copper per phase of the generator.

Phase Discriminator

Armature Current Detector

By sensing a voltage proportional to a motor phase current, one can determine the location of the armature magnetic axis. This can be seen by examination of Figure BII. From Section 4.1.4 of [25], the radial flux density of an armature winding is directly proportional to the amplitude of the current in that winding. Therefore, using symmetry and the configuration of Figure BII (a), it is seen that the magnetic axis of the armature rotates in phase with the phase 1 current and as shown in Figure BII (c).

Rotor Field Detector

The Hall voltage is shown in Figure BIII (b). H is the Hall constant. For a discussion of the Hall effect see [1].

When the armature current detection voltage is in phase with the Hall voltage, $\alpha = -90^{\circ}$. This and other relationships of rotor and armature are shown in Figure BIV. Voltages are not necessarily of the same amplitude as shown here.

Crash Astern Energy Calculation

Using Figure II, the deceleration torque is determined from the model curve. Power is calculated as follows:

$$\left(\frac{Q}{\rho D^5}\right) \times 2\rho D^5 = Q_{P\ \text{total}}$$

$$2\pi n\, Q_{P\ \text{total}} = \text{Total Power} \qquad \text{(B2)}$$

Figure BII

(a) Armature Configuration
(b) 3-phase currents
(c) Magnetic axis position at varying ωt.

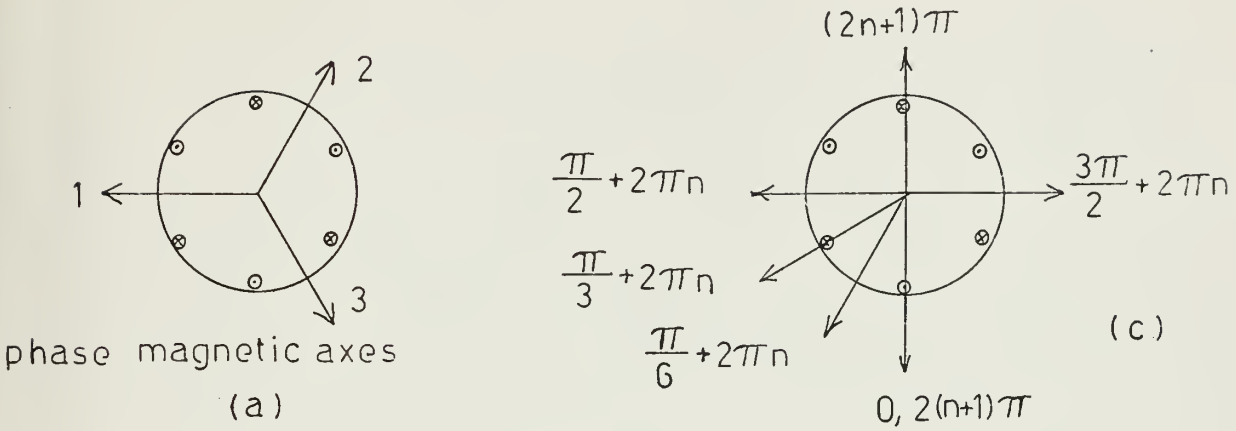

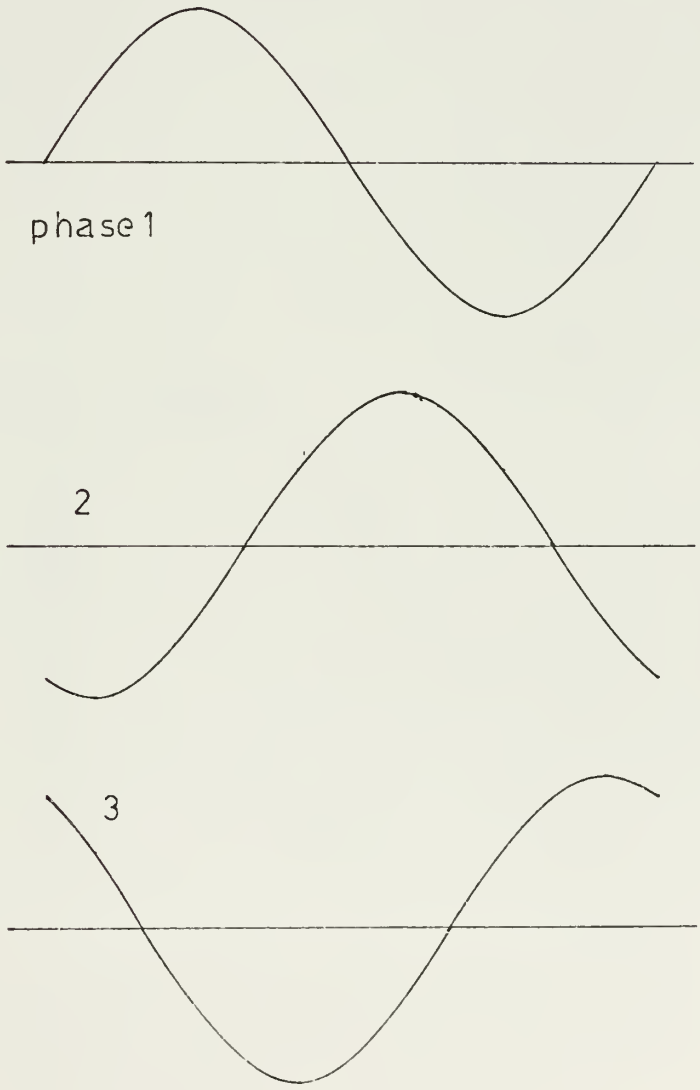

Figure BIII

(a) Rotor Configuration
(b) Hall voltage induced by various positions of rotor point A.

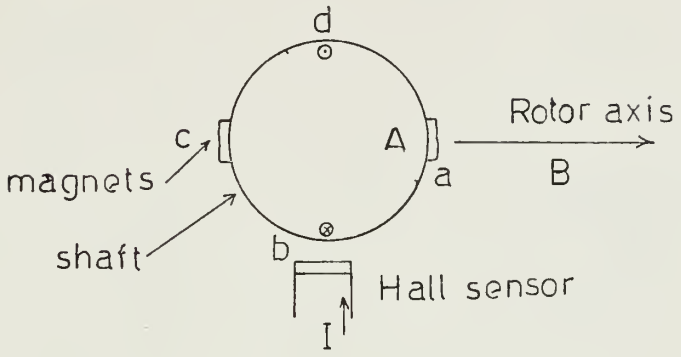

(a)

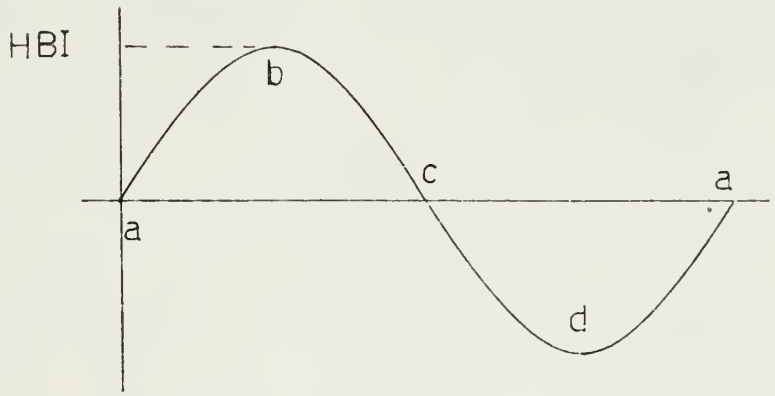

(b)

Figure BIV

Voltage waveforms and corresponding magnetic axes positions for (a) $\alpha = -90^{o}$, (b) $\alpha = -60^{o}$, (c) $\alpha = -120^{o}$.

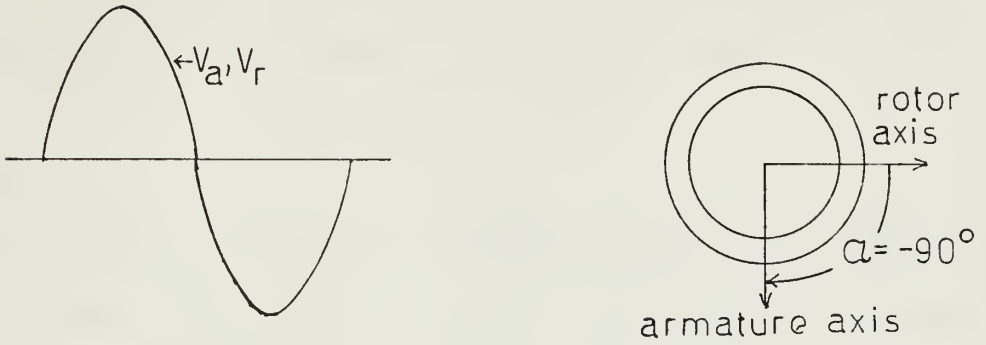

(a)

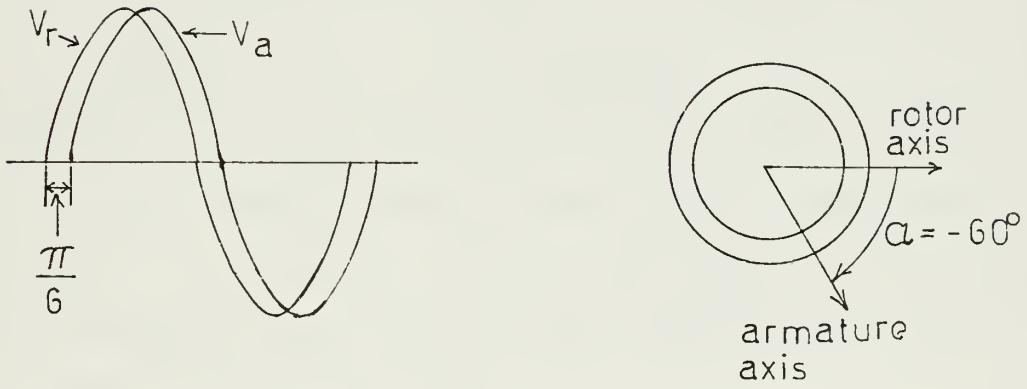

(b)

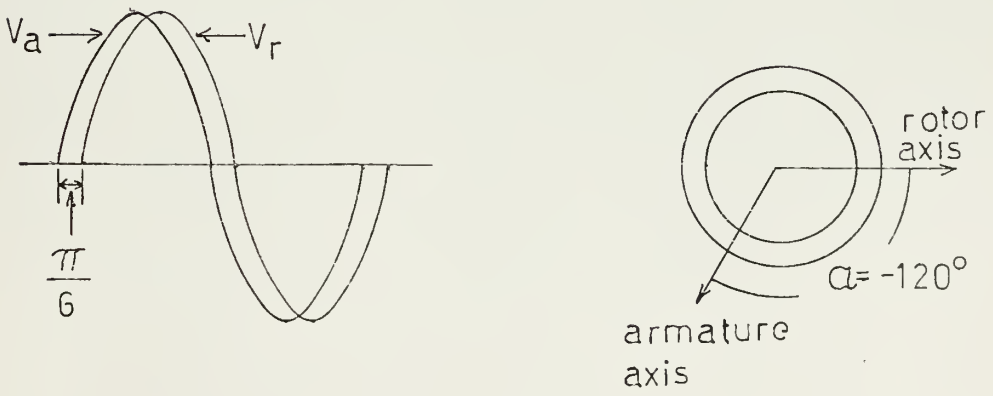

(c)

Figure VIII gives n versus t. Knowing n and v allows use of Figure II to obtain torque. Equation (B2) is plotted against time in Figure BV. Integrating this curve graphically yields hydrodynamic energy to be dissipated by the braking resistor. The integral yields 10.4×10^6 joules.

Refrigeration

From [19], Table I, one can get an approximate idea of the refrigeration needs for the plant. For a machine rating of 10,000 KW, the low temperature (4.2°K) cooling load is 29.9 watts. For this plant, there are two motors and two generators requiring cooling at 4.2°K. These are rated at about 26,100 KW each. For a rough estimate, the load for this plant is:

$$4\left(\frac{26.1}{10.}\right)\ 29.9 \overset{\sim}{=} 4(3)\ (30) = \underline{360 \text{ watts}}$$

Using Figures 6 and 7 of [22], installed and hourly direct operating costs can be obtained. Installed costs are about $\$3 \times 10^5$. Hourly operating costs are about \$23. This cost data is an estimate based on extrapolation of cost data from existing smaller units. However, the building of such a large unit is within the state of the art.

Figure BV

Energy Dissipation in Crash Astern

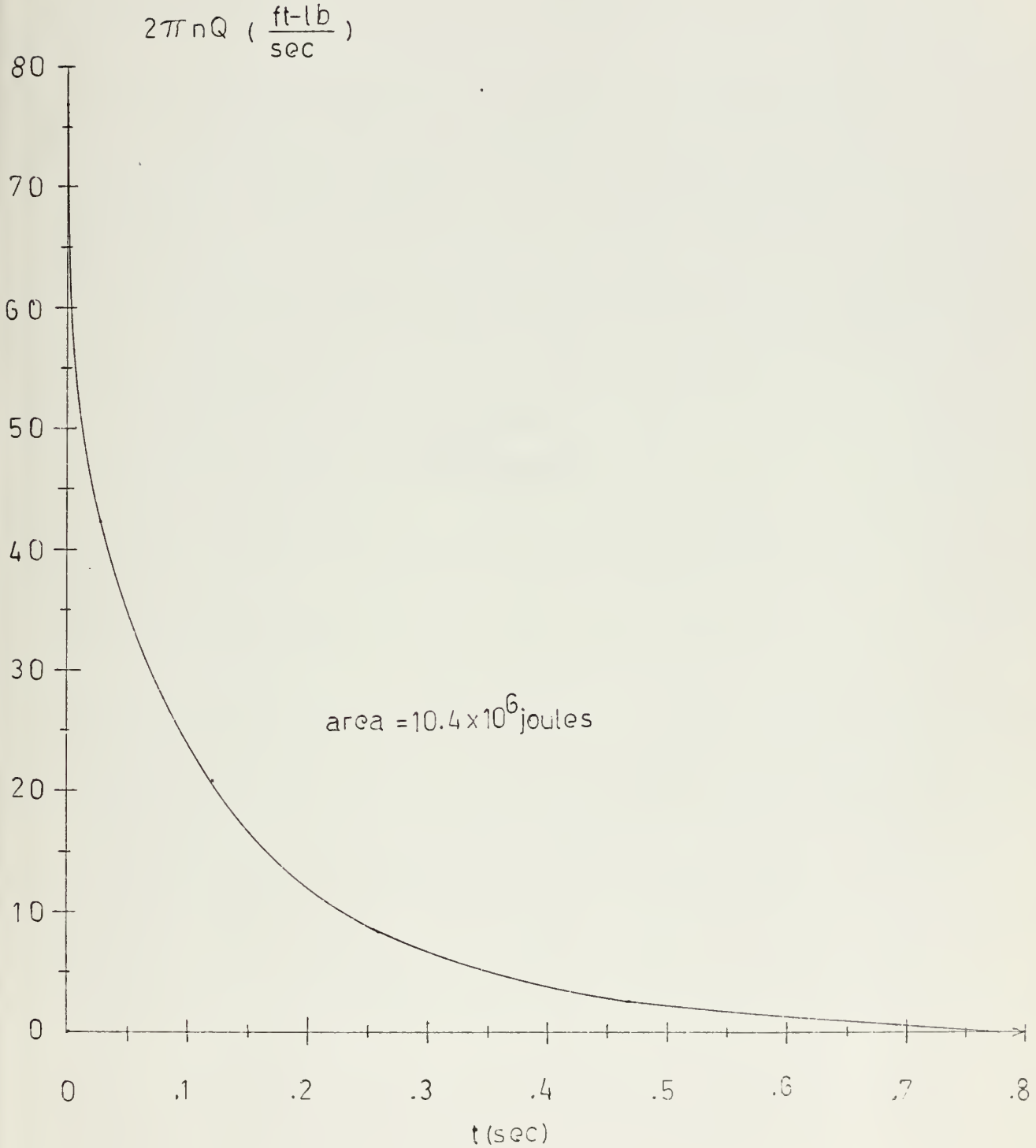

APPENDIX C

BIBLIOGRPAHY

1. Adler, R. B., Smith, A. C., Longini, R. L., Introduction to Semiconductor Physics, John Wiley & Sons, Inc., New York, 1964, pp. 55-56.

2. Amato, C. J., "An AC Equivalent Circuit for a Cycloconverter", IEEE Transactions on Industry and General Applications, Sept/Oct 1966.

3. Boatwright, G. M., Turner, J. J., "Effect of Ship Maneuvers on Machinery Component Design", Bureau of Ships Journal, Sept., 1965.

4. Burford, H. M., Koch, R. L., Westbrook, J. D., "Performance of a Diesel Electric A.C. Propulsion Plant Based on the Design and Sea Trials of U.S.S. Hunley (AS-31)", SNAME, Hampton Roads Section, Oct. 1962.

5. Comstock, J. P., ed., Principles of Naval Architecture, Society of Naval Architects and Marine Engineers, New York, 1967, pp. 441-442.

6. Gibson, J. E., Tuteur, F. B., Control System Components, McGraw Hill, 1958, pp. 254-259.

7. Gold, P. D. Jr., Lcdr, USN, "Stopping and Backing Trials of a Destroyer", JASNE, Vol. 53, No. 1, Feb., 1941.

8. Greeneisen, D. P., "A Design Program for Superconducting Electrical Machines", SM thesis in preparation, Massachusetts Institute of Technology (1968).

9. Griffith, D. C., Ulmer, R. M., "A Semiconductor Variable Speed A-C Motor Drive", Electrical Engineering, May, 1961, pp. 350-353.

10. Lewis, J. W., Scoville, F. W., Lecourt, E. J., "United States Coast Guard Icebreaker Propulsion System Simulation", Phases 1 and 2, Sept-Oct, 1967, USCG Office of Engineering, Icebreaker Design Branch.

11. Majmudar, Harit, Electromechanical Energy Converters, Allyn and Bacon, Boston, 1965, pp. 350-384.

12. Markus, John, ed., Handbook of Electronic Control Circuits, McGraw Hill, 1959, p. 131.

13. Miniovich, I. Y., "Investigation of Hydrodynamic Characteristics of Screw Propellers under Conditions of Reversing and Calculation Methods for Backing of Ships", Bureau of Ships Translation No. 697.

14. Nordstrom, H. F., "Screw Propeller Characteristics", Publications of the Swedish State Shipbuilding Experimental Tank, No. 9, N. J. Gumperts Bokhandel A. B., Goteberg, 1948.

15. Partridge, G. R., Principles of Electronic Instruments, Prentice-Hall, Inc., Englewood Cliffs, N. J., 1958.

16. Seward, H. L. ed., Marine Engineering, Vol. I, Society of Naval Architects and Marine Engineers, New York, 1944, p. 293.

17. Sibley, E. H., Frankel, E. G., Reynolds, J. M., "Superconductivity: Status and Implications for Marine Applications", SNAME, Marine Power Plant Symposium, Phila., Pa., May 11-13, 1966, paper no. 8.

18. Slabiak, W., Lawson, L. J., "Precise Control of a Three-Phase Squirrel-Cage Induction Motor Using a Practical Cycloconverter", IEEE Transactions on Industry and General Applications, July/August, 1966.

19. Stekly, Z. J. J., Woodson, H. H., "Rotating Machinery Utilizing Superconductors", IEE Transactions on Aerospace, vol. 2, No. 2, April 1964, pp 826-842.

20. Terman, F. F., Pettit, J. M., Electronic Measurements, McGraw Hill, 1952, pp 272-275.

21. Thau, W. E., "Propellers and Propelling Machinery, Maneuvering Characteristics during Stopping and Reversing", Trans. SNAME, Vol. 45, 1937, pp 124-144.

22. Timmerhaus, K. D., ed., Advances in Cryogenic Engineering, Vol. 11, Plenum Press, N. Y., 1966, pp 122-125.

23. Truxal, John G., ed., Control Engineers' Handbook, 1st ed., McGraw-Hill Book Co., Inc., New York, 1958.

24. Van Eck, R. A., "Frequency-Changer Systems Using the Cycloconverter Principle", AIEE Trans., Applications and Industry, May, 1963, pp 163-168.

25. Woodson, H. H., Melcher, J. R., Electromechanical Dynamics, Part II, Dept. of Electrical Engineering, Massachusetts Institute of Technology, January, 1967.